Aus dem klinischen Forschungszentrum des Exzellenzclusters
NeuroCure der Medizinischen Fakultät
Charité – Universitätsmedizin Berlin

DISSERTATION

Pathophysiologisch-serologische, bildgebende und klinische Charakteristika der Neuromyelitis Optica

zur Erlangung des akademischen Grades
Doctor medicinae (Dr. med.)

vorgelegt der Medizinischen Fakultät
Charité – Universitätsmedizin Berlin

von

Sophie Schumacher

aus Güstrow

Datum der Promotion: 23. Juni 2019

Inhaltsverzeichnis

Abkürzungsverzeichnis

ADEM	Akute disseminierte Enzephalomyelitis
AQP-4-Ak	Aquaporin-4-Antikörper
FLASH	Fast Low Angle Shot
HC	Gesunde Kontrollen engl: healthy controls
logMAR	Logarithmus der “Minimum Angle of Resolution”
MOG-Ak	Myelin-Oligodendrozyten-Glykoprotein-Antikörper
MRT	Magnetresonanztomografie
MS	Multiple Sklerose
NMOSD	Neuromyelitis optica-Spektrum-Erkrankungen englisch: Neuromyelitis optica spectrum diseases
OCT	Optische Kohärenztomografie englisch: Optical Coherence Tomography
ON	Optikusneuritis
pRNFL	Peripapilläre retinale Nervenfaserschicht englisch: peripapillary nerve fiber layer
PVA	Periventrikuläre Venendichte englisch: Periventricular venous area
SWI	Suszeptibilitätsgewichtete Bildgebung englisch: Susceptibility weighted imaging
T	Tesla
UHF-MRT	Ultrahochfeld-Magnetresonanztomografie
VEP	Visuell Evozierte Potenziale

1. Zusammenfassung

1.1 Abstrakt

Hintergrund: *Neuromyelitis optica-Spektrum-Erkrankungen* (NMOSD) stellen eine Gruppe neuroinflammatorischer Erkrankungen dar, die mit dem klinischen Auftreten von Myelitiden und/oder Optikusneuritiden (ON) einhergeht. Aufgrund zahlreicher überlappender klinischer und paraklinischer Eigenschaften beim Nachweis verschiedener Antikörper, vor allem auch in Abgrenzung zur Multiplen Sklerose (MS), besteht weiterhin der Bedarf nach neuen Biomarkern.

Methodik: In zwei Studien wurden NMOSD-Patienten mit positivem Nachweis für Aquaporin-4-Antikörper (AQP-4-Ak) mittels 7 Tesla (T) Magnetresonanztomografie (MRT) hinsichtlich der I) periventrikulären Venendichte (PVA) in T2*-gewichteten Aufnahmen und II) der Phasenverschiebung in suszeptibilitätsgewichteten Sequenzen untersucht. Als Vergleich dienten die Ergebnisse von Patienten mit MS und gesunden Kontrollen (HC). In einer dritten Arbeit (III) erfolgte eine retrospektive Auswertung visueller Parameter im Vergleich von AQP-4-Ak-positiven Patienten und Patienten mit Antikörpern gegen das Myelin-Oligodendrozyten-Glykoprotein (MOG) mittels Optischer Kohärenztomografie (OCT), Visuell Evozierter Potenziale (VEP) und der Fernvisus-Messung.

Ergebnisse: Bildmorphologisch zeigte sich in den 7T-T2* gewichteten Aufnahmen bei Patienten mit AQP-4-Ak-positiver NMOSD eine normal große PVA (AQP-4-Ak: PVA = 133 mm^2; MS: PVA = 117 mm^2; HC: PVA =144 mm^2) und überwiegend fehlende paramagnetische Phasenverschiebungen (107 von 112 Läsionen, 96%) in den SWI-Sequenzen. Hinsichtlich des Vergleichs von MOG-Ak- gegenüber von AQP4-Ak-positiven Patienten fiel eine größere absolute Schubrate (Mittelwert, Spannweite, MOG-Ak: 4.5, 1 - 13; APQ4-Ak: 2, 1 -4; p = 0.012), bei insgesamt ähnlichem Verlust der im OCT gemessenen peripapillären retinalen Nervenfaserschicht (pRNFL) der AQP-4-Ak-positiven NMOSD im Vergleich zu den MOG-Ak-positiven Patienten auf (Mittelwert ± Standardabweichung, MOG-Ak: 59 ± 23 µm, AQP-4-Ak: 59 ± 21 µm). Jedoch waren die Werte der pRNFL nach dem Erstereignis einer ON bei den Patienten mit AQP-4-Ak deutlich stärker reduziert, als bei den MOG-Ak-positiven Patienten (AQP-4-Ak: pRNFL-Verlust = 32.8 μm ($p<0.001$); MOG-Ak: pRNFL-Verlust = 12.8 μm ($p=0.001$)).

Schlussfolgerung: Mit Hilfe von modernen diagnostischen Verfahren, wie dem Ultrahochfeld-MRT und dem OCT wird die bessere Charakterisierung von phänotypisch ähnlichen neuroinflammatorischen Krankheitsentitäten ermöglicht. Die hierfür zugrundeliegenden

unterschiedlichen Pathomechanismen sind bisher nicht vollständig verstanden und bedürfen weiterer Untersuchungen.

1.2 Abstract

Introduction: Different neuroinflammatory entities define the group of *Neuromyelitis optica spectrum disorders* (NMOSD) and are usually associated with the presentation of myelitis and/or optic neuritis. Although various antibodies were verified, there is still the challenge of overlapping clinical and paraclinical phenotypes which ask for further new diagnostic parameters.

Methods: By using 7 Tesla (T) magnetic resonance imaging (MRI) patients with aquaporin-4-antibodies (AQP-4-ab) were investigated concerning a) the periventricular venous area (PVA) at T2*-weighted images and b) the phase changes within brain lesions at susceptibility-weighted (SWI)-images. The findings were compared to patients with Multiple Sclerosis (MS) and healthy controls (HC). Further patients with AQP-4-ab and antibodies against myelin oligodendrocyte glycoprotein (MOG-ab) were faced by using retrospective data of retinal optical coherence tomography (OCT), visual acuity and visual evoked potentials (VEP).

Results: Patients with AQP-4-ab presented equal results like HC concerning the PVA (AQP-4-ab: PVA = 133 mm^2; MS: PVA = 117 mm^2; HC: PVA =144 mm^2) and predominantly missing phase changes in brain lesions at SWI-images (107 of 112 lesions, 96%). Both, AQP-4-ab- and MOG-ab-positive patients, presented a loss in peripapillary nerve fiber layer (pRNFL) thickness at the same extend (mean ± standard deviation, MOG-ab: 59 ± 23 µm, AQP4-ab: 59 ± 21 µm), while the number of episodes of optic neuritis (ON) was lower in AQP4-ab-positive patients (mean, range, MOG-ab: 4.5, 1 - 13; APQ4-ab: 2, 1 -4; p = 0.012). However, the loss of pRNFL thickness after the first episode of ON was greater in patients with AQP-4-ab (AQP-4-ab: pRNFL-loss = 32.8 μm ($p<0.001$); MOG-ab pRNFL-loss = 12.8 μm ($p=0.001$).

Conclusion: With the help of novel diagnostic tools, like the ultrahighfield-MRI and OCT, it is possible to distinguish between neuroinflammatory entities with similar phenotypes. For a better understanding of the underlying pathomechanisms further investigations are still needed.

1.3 Einführung

Neuromyelitis optica spectrum disorders (NMOSD), im deutschsprachigen Raum *„Neuromyelitis optica-Spektrum-Erkrankungen",* umfasst eine Gruppe von neuroinflammatorischen Autoimmunerkrankungen, welche klinisch durch das Auftreten schwerer Myelitiden und/oder Optikusneuritis (ON) gekennzeichnet sind. Differentialdiagnostisch lassen sich bei der Mehrzahl der Patienten Antikörper gegen Aquaporin-4 (AQP-4-Ak) im Serum nachweisen [1, 2]. Vor allem die Ähnlichkeit des klinischen Phänotyps von NMOSD und der Multiplen Sklerose (MS) [1] führt immer wieder zu Fehldiagnosen in der klinischen Routine [3-13], obwohl es sich bei der NMOSD immunpathogenetisch von der MS distinkte Erkrankung handelt [14-17]. Da sich aber die Therapiestrategien der beiden Erkrankungen unterscheiden [3, 18-23], ist die sichere diagnostische Abgrenzung von entscheidender Bedeutung.

Die Darstellung von zerebralen Läsionen und deren Charakterisierung ist mit Hilfe von Ultrahochfeld-Magnetresonanztomografie (UHF-MRT) mit einer Feldstärke von 7 Tesla (T) in einer höheren Detailschärfe möglich [24]. Im Detail können am Rand zahlreicher MS-Läsionen hypointense ringartige Strukturen auf T2*-gewichteten Aufnahmen und intraläsionale, im Zentrum der MS-Läsion gelegene, Venen detektiert werden [25, 26]. Diese für MS nahezu pathognomische Morphologie [27] konnte nur bei wenigen NMOSD-Läsionen gesehen werden [25, 26]. Ebenso geht die Darstellung von zerebralen Venen bei UHF-MRT-Aufnahmen des Zerebrums von MS-Patienten mit einer reduzierten Sichtbarkeit einher [28, 29]. Als Erklärung hierfür wird eine geringere Sauerstoffausschöpfung des Blutes durch vorausgegangene Umbauprozesse, wie Gliose, und der damit einhergehende hypometabolische Status angenommen. Die dadurch geringere Desoxygenierung des Blutes im venösen System führt zu verringerten suszeptibilitätsabhängigen Signalverlusten in den T2*-gewichteten Bildern [28, 29].

Da ein Teil der AQP-4-Ak-negativen NMOSD-Patienten, aber auch eine kleine Gruppe von MS-Patienten, sowie Patienten mit akut disseminierter Enzephalomyelitis (ADEM) Antikörper gegen das Myelin-Oligodendrozyten-Glykoprotein (MOG) im Serum zeigen [30-36], wird aktuell diskutiert, ob diese MOG-Ak-positiven Patienten mit klinischem NMOSD-Phänotyp als NMOSD oder als eigene Krankheitsentität eingeteilt werden sollte [37-39]. Die klinische Symptomatik dieser Patienten ist ebenso wie bei AQP-4-Ak-positiven Patienten durch ON und (rekurrente) transverse Myelitis charakterisiert [40]. Unterschiedlich sind dabei die Zielzellen der Antikörper: MOG-Ak interagieren mit Oligodendrozyten, AQP4-Ak mit Astrozyten.

Die ON verlaufen bei NMOSD-Patienten meist schwerwiegend und gehen mit einer deutlichen Visusminderung, bishin zur Blindheit, und einem Verlust von retinalen Nervenfasern und

Ganglionzellen einher [41-44]. Meist sind dabei beide Augen betroffen [5, 41], und die visuelle Lebensqualität ist signifikant reduziert [45]. Bei bis zu 20% der betroffenen Augen lassen sich makuläre Mikrozysten als Ausdruck eines gravierenden retinalen Schadens in der inneren Körnerschicht finden [46-48]. Das Krankheitsbild der MOG-Ak-assoziierten Enzephalomyelitis mit ON ist zum jetzigen Zeitpunkt noch nicht abschließend klinisch charakterisiert. Vermutlich kommt es bei Patienten mit dem Nachweis von MOG-Ak im Serum zu multiphasischen Verläufen der Erkrankung [30] mit einem geringen Ausmaß an verbleibenden neuro-axonalen retinalen Schäden [40, 49, 50].

Ziel der im Anschluss dargestellten Studien war die Gegenüberstellung der bildmorphologischen Analyse der AQP-4-Ak-positiven NMOSD gegenüber der MS, als auch die visuell-klinischen Unterschiede zwischen MOG-Ak und AQP-4-Ak-positiven Patienten. Dabei liegt der Fokus dieser Arbeit in der besseren Abgrenzung der hier dargestellten verschiedenen neuroimmunologischen Krankheitsentitäten und die daraus resultierende Therapieentscheidung mit der damit verbundenen großen klinischen Relevanz.

1.4 Methodik

Probanden:

Projekt I) Untersucht wurden die hochaufgelösten 7T T2*-gewichteten Aufnahmen von 16 NMOSD-Patienten [1] mit positivem Nachweis von AQP-4-Ak im Serum. Als Kontrollen dienten 16 Patienten mit schubförmig-remittierender MS und 16 gesunde Kontrollen (HC) [51].
Projekt II) Weiterhin wurden in einer Querschnittsstudie 10 NMOSD-Patienten [1] und 10 Patienten mit schubförmig-remittierender MS zunächst hinsichtlich unterschiedlicher Muster von intraläsionalen Suszeptibilitäts-assoziierten positiven Phasen-Verschiebungen verglichen [52].
Projekt III) Im Rahmen einer retrospektiven Multizenterstudie (fünf deutsche Zentren: Berlin, Freiburg, Düsseldorf, Heidelberg, Würzburg; ein dänisches Zentrum: Vejle) wurde das Ausmaß des Retinaschadens, verursacht durch ON, in betroffenen Augen von 16 Patienten mit MOG-Ak-assoziierter Enzephalomyelitis mit ON analysiert [53]. Hierzu wurden die Daten verschiedener Untersuchungen des visuellen Systems (Optische Kohärenztomografie (OCT), Sehschärfe, Visuell Evozierte Potenziale (VEP)) mit denen von 16 Patienten mit AQP4-Ak-positiven NMOSD-Patienten mit ON und 16 Kontrollen verglichen. Dabei wurden Augen aus den statistischen Analysen ausgeschlossen, die ophthalmologische Komorbiditäten aufwiesen oder innerhalb der letzten drei Monate eine ON präsentierten.

Die hier dargestellten Studien wurden von der lokalen Ethikkommission genehmigt und nach den Grundsätzen zur Sicherung Guter Wissenschaftlicher Praxis der Charité – Universitätsmedizin Berlin und den geltenden Gesetzen der Bundesrepublik Deutschland durchgeführt. Alle Studienteilnehmer wurden ausführlich aufgeklärt und erteilten schriftliches Einverständnis.

MRT-Bildgebung:

Die UHF-MRT-Aufnahmen für Projekt I und II wurden mit einem 7T Magnetom von Siemens zusammen mit einer 24-Kanal-Kopfspule von der Firma „Nova Medical“ gemessen. Das Sequenzprotokoll beinhaltete eine zweidimensionale T2*-gewichtete Fast Low Angle Shot (FLASH) acquisition Sequenz mit einer räumlichen Auflösung von $0.5 \times 0.5 \times 2$ mm^3, einer Echozeit von 25.0 ms, einer Repetitionszeit von 1,820 ms und einem Anregungswinkel (flip angle) von 35°. Dabei betrug die Schichtdicke 2 mm. Ebenfalls wurde eine zweidimensionale fluid attenuated inversion recovery Sequenz mit einer räumlichen Auflösung von (1.0×1.0) mm^2, einer Echozeit von 90 ms, einer Repetitionszeit von 16000 ms, einer Inversionszeit von 2925.5 ms bei einer Schichtdicke von 3 mm gemessen. Das Untersuchungsprotokoll beinhaltete ferner eine dreidimensionale Gradienten-Echo, flusskompensierte suszeptibilitätsgewichtete Sequenz (SWI) mit einer räumlichen

Auflösung von 0.5 × 0.5 × 1 mm^3, einer Echozeit von 14 ms, einer Repititionszeit von 25 ms und einem Anregungswinkel (flip angle) von 12°. Die Sequenz beinhaltete die Messung von Magnitude- und gefilterte Phasenbilder aus denen dann die finalen SWI-Daten berechnet wurden.

MRT-Bildauswertung:

Zur Bildanalyse und Nachbearbeitung der UHF-MRT-Aufnahmen wurde das Programm OsiriX [54] Version 3.8.1 verwendet.

Analyse der Anzahl an Läsionen und der periventrikulären Venendichte (PVA)

Die Analyse der 7T MRT-Sequenzen erfolgte manuell durch einen für alle klinischen Daten verblindeten Beobachter. Eine Hyperintensität mit einem Durchmesser größer als 3 mm wurde als Läsion gezählt. Die periventrikuläre vaskuläre Fläche in mm^2 wurde als Marker für die PVA mittels eines festen Algorithmus ermittelt. Hierzu wurde die Minimumintensitätsprojektion aus zwei benachbarten axialen T2*-gewichteten Schichten genutzt. Dies verbesserte die Darstellung des vollständigen Venenverlaufs.

Vergleichende Analyse des intra- und periläsionalen Phasenverschiebung in T2-gewichteten und SWI-Sequenzen*

Die 7T MRT-Sequenzen der beiden Protokolle wurden hinsichtlich der klinischen Daten verblindet ausgewertet. Die in den T2*-gewichteten Aufnahmen markierten Hyperintensitäten mit einem Durchmesser größer als 3 mm wurden in den suszeptibilitätsgewichteten Bildern aufgesucht und bezüglich ihrer erkennbaren Phasenverschiebung in vier verschiedenen Subtypen eingeteilt: i) runde Läsionen mit nachweislich zentraler paramagnetischer Phasenverschiebung ii) Läsionen mit ringförmiger paramagnetischer Phasenverschiebung iii) Läsionen ohne paramagnetischer Phasenverschiebung iiii) Läsionen mit paramagnetischer Phasenverschiebung, der nicht den vorherigen Subtypen zuordenbar, also „unspezifisch“, ist. Erkennbare, durch ein Gefäß hervorgerufene paramagnetische Phasenverschiebungen gingen dabei nicht in die Auswertung mit ein.

Nachweis einer zentralen Vene innerhalb von Läsionen

Die in den T2*-gewichteten Sequenzen der hochaufgelösten MRT-Aufnahmen festgelegten Läsionen wurden hinsichtlich des Auftretens einer zentralen Vene untersucht. Dabei galt eine Vene als zentral, sobald sie im inneren Drittel der Läsion lokalisiert war.

Untersuchungen des visuellen Systems:

Die klinischen Daten sowie Untersuchungsergebnisse für Projekt III (OCT, VEP, Sehschärfe) wurden retrospektiv analysiert.

OCT

Die Untersuchung aller Patienten erfolgte am jeweiligen Zentrum mittels eines Spectralis SD-OCT Gerät (Heidelberg Engineering, Heidelberg, Deutschland). Die pRNFL wurde in einem Ringscan (12°, 768 oder 1536 A-scans, 16≤ART≤100) um den Nervus opticus herum gemessen. Das Makulavolumen wurde an jedem Zentrum mit ähnlichen Scans erfasst (25°×30°, 61 vertikale oder horizontale B-scans, 768 A-scans pro B-scan, 9≤ART≤15). Die Auswertung erfolgte zentral mittels der geräteinternen Software Eye Explorer Software, Version 1.9.10.0 mit dem Viewing Module 6.0.9.0.

VEP

Alle Patienten und Kontrollen wurden mittels der VEP-Untersuchung durch Schachbrettmuster-Stimulation (1°) untersucht. Die Latenzzeit (P100) wurde als abnormal eingeordnet, sobald sie länger als 112ms [55] betrug oder wenn kein eindeutiges Signal gemessen werden konnte.

Fernvisus

Die Sehschärfe der Patienten wurde mit Buchstaben-Sehtafeln gemessen und anschließend in die Einheit ‚logMAR' umgerechnet. Eine Sehschärfe von 0,2 logMAR und schlechter wurden als abnormal gewertet. Das reine Erkennen der Anzahl der Finger ergab einen Wert von 2,0 logMAR, das Erkennen von Handbewegungen entsprach 3,0 logMAR.

Statistische Analyse:

Die statistische Auswertung erfolgte mit Hilfe von Statistical Package for Social Science (SPSS, Version 22, IBM, Armonk, New York, USA) und dem Programm R [56] Version 3.1.2 mit den Paketen psych, MASS, geepack und ggplot. P-Werte kleiner als 0,05 wurden als signifikant gewertet. Die Unterschiede zwischen den Gruppen (NMOSD, MS, Kontrollen) hinsichtlich der PVA wurden mittels des parametrischen Student *t* Tests analysiert. Mittels Mann – Whitney U Test wurden die Unterschiede des intraläsionalen Phasenwechsels zwischen MS- und NMOSD-Patienten untersucht. Die Ergebnisse der visuellen Untersuchungen der MOG-Ak und AQP-4-Ak-positiven Patienten wurden durch verallgemeinerte Schätzgleichungen („generalized estimating equation") analysiert, die die Inter-Augen-Abhängigkeiten eines Probanden berücksichtigen. Weitere Details zu den verwendeten Tests sind den jeweiligen Originalarbeiten zu entnehmen.

1.5 Ergebnisse

Bildmorphologische Unterschiede:

Vergleich der PVA bei NMOSD und MS:

Die Auswertung bei den Patienten mit NMOSD ergab eine durchschnittliche PVA von 133 mm^2 (Mittelwert ± Standardabweichung, Spannweite; 133 ± 21, 98 – 170 mm^2) und war damit nicht signifikant kleiner als bei den HC (Mittelwert ± Standardabweichung, Spannweite; 144 ± 27, 92 - 202 mm^2; $p = 0.226$). Im Gegensatz dazu zeigten die Patienten mit MS eine signifikant verkleinerte periventrikuläre Venendichte (Mittelwert ± Standardabweichung, Spannweite; 117 ± 30, 61 – 173; $p = 0.013$). Weiterhin verhielten sich die Anzahl der zerebralen Läsionen und die periventrikuläre Venendichte bei den MS-Patienten indirekt proportional zueinander ($r_s = -0.555$, $p = 0.026$). Dies konnte bei den NMOSD-Patienten nicht beobachtet werden.

Beurteilung der Phasenverschiebung:

In der untersuchten Kohorte ließen sich insgesamt 112 Läsionen bei 10 NMOSD-Patienten und 232 Läsionen bei 10 MS-Patienten in supratentoriellen T2*-gewichteten FLASH-Bildern bei einer Feldstärke von 7T detektieren. Davon zeigten 32 (14%) der MS-Läsionen eine zentrale und 75 (32%) eine ringförmige Phasenverschiebung in den SWI-Sequenzen. Somit konnten 46% der MS-Läsionen den Subtypen i) für zentrale und ii) für ringförmige Phasenverschiebungen zugeordnet werden. Dem gegenüberstehend konnten nur 2% der Läsionen von NMOSD-Patienten diesen beiden Subtypen zugeordnet werden. Der überwiegende Anteil der Läsionen von NMOSD-Patienten zeigte keine paramagnetische Phasenverschiebung (107 von 112 Läsionen, 96%) und gehört damit dem Subtyp iii), also Läsionen ohne sichtbare Phasenverschiebung in den SWI-Sequenzen, an. Unter den Läsionen von MS-Patienten betrug dieser Anteil 50% (116 von 232 Läsionen).

Häufigkeit zentraler Venen in Hirnläsionen

Ein Großteil der Läsionen von MS-Patienten (193 der 232 Läsionen, 83%) präsentierten innerhalb des inneren Drittels eine zentrale Vene und grenzten sich dadurch von der Morphologie der Läsionen von NMOSD-Patienten ab; bei ihnen ließen sich nur in 25% der Fälle (28 der 112 Läsionen) eine zentrale Vene nachweisen.

Ergebnisse der Untersuchungen des visuellen Systems:

Anzahl der ON

Gemessen an der absoluten Schubrate an ON zeigte sich eine größere Anzahl an ON bei Patienten mit MOG-Ak im Vergleich zu denen mit AQP-4-Ak (Mittelwert, Spannweite, MOG-Ak: 4.5, 1 - 13; APQ4-Ak: 2, 1 -4; p = 0.012).

OCT

Die Dicke der pRNFL in beiden Patientengruppen im Vergleich zur Gruppe der HC erniedrigt (Mittelwert ± Standardabweichung; MOG-Ak: 59 ± 23 µm, AQP-4-Ak: 59 ± 21 µm, HC: 99 ± 6 µm, p < 0,001). Beim direkten Vergleich der beiden Patientengruppen bestand kein signifikanter Unterschied in der pRNFL-Dicke (p = 0.94). Der Verlust der pRNFL nach nur einer ON bei Patienten mit positivem Antikörpernachweis für MOG-Ak betrug durchschnittlich 12.8 µm. Bei Patienten mit AQP-4-Ak belief sich dieser Verlust auf 32.8 µm (p = 0.001). Weiterhin waren innerhalb beider Gruppen makuläre Mikrozysten in der inneren Körnerschicht der von ON betroffenen Augen nachweisbar (MOG-Ak: 5 Augen mit Mikrozysten (21.7%), AQP-4-Ak: 4 Augen mit Mikrozysten (19.0%)).

VEP

In der Gruppe der Patienten mit MOG-Ak ließen sich bei 12 Augen von 20 Augen nach ON (60%) eine abnormale P100-Latenz von über 112 ms nachweisen. Dies war in vergleichbarer Häufigkeit bei 10 von 20 Augen (50%) der Patienten mit AQP-4-Ak festzustellen.

Fernvisus

Bei Patienten mit MOG-Ak war die Sehschärfe einerseits im Durchschnitt bei allen ON-betroffenen Augen reduziert (Mittelwert ± Standardabweichung; 0,35 ± 0,88 log MAR) und 3 Augen zeigten sich komplett blind (logMAR ≥ 1,0). Andererseits waren bei 16 der 23 von ON betroffenen Augen eine Sehschärfe von mindestens 0,1 logMAR erhalten. Im Gegensatz dazu ergab die Sehschärfetestung bei den Patienten mit AQP-4-Ak schlechtere Werte (Mittelwert ± Standardabweichung; 0,72 ± 1,09 logMAR). Allerdings zeigte sich der Unterschied der Sehschärfe zwischen den Patientengruppen als nicht signifikant (p=0,3).

1.6 Diskussion

Mit Hilfe von modernen Technologien lassen sich heutzutage vielerlei Erkrankungen bereits *in vivo* besser verstehen und diagnostizieren. Die UHF-MRT ermöglicht, im Vergleich zu konventionellen MRT-Sequenzen (1.5 T), durch das hohe Signal-Rausch-Verhältnis und den stärker ausgeprägten Suszeptibilitätseffekten eine deutlich verbesserte Darstellbarkeit zerebraler Strukturen [24, 57-59]. Ebenso bedeutend ist die Darstellung oberflächlicher, anatomischer Strukturen in Echtzeitmessung mittels der OCT [60, 61]. Weitere visuelle Parameter, wie VEP und die Sehschärfetestung erweitern die Erkenntnisse bezüglich der Pathogenese der NMOSD [62]. Der fortwährende Antrieb für neue Studien ergibt sich durch weiterhin bestehende Unsicherheiten in der Abgrenzung innerhalb der diversen neuroinflammatorischen Krankheitsentitäten.

Aufgrund der klinischen Ähnlichkeiten war man früher der Auffassung, dass es sich bei der Neuromyelitis optica und der MS um eine Krankheitsentität handelt. Diese Annahme konnte durch neue Erkenntnisse mittels MRT-Bildgebung und dem Nachweis von Antikörpern gegen den Wasserkanal Aquaporin-4 im Serum widerlegt werden [63-65]. Wir wissen heute, dass von einer eigenen Krankheitsentität der NMOSD auszugehen ist, die sich hinsichtlich des Pathomechanismus von der MS abgrenzt [66]. Auch die Therapieoptionen sind andere [67]: viele der bei der MS gegebenen Immunmodulatoren sind bei der NMOSD unwirksam oder sogar schädlich [4, 21, 23, 68, 69]. Um pathophysiologische Unterschiede in vivo herauszuarbeiten haben wir im Rahmen unserer Untersuchungen die Dichte der periventrikulären Venen bei Patienten mit NMOSD analysiert und mit den Ergebnissen von Patienten mit MS und HC verglichen. Die Sichtbarkeit der venösen Gefäße in der MRT-Bildgebung ist dabei von verschiedenen Faktoren abhängig. Hierzu zählen die Flussgeschwindigkeiten des Blutes, der Durchmesser der Gefäße und das magnetische Verhalten des Hämoglobins entsprechend seines Oxygenierungsgrades. Desoxygeniertes Hämoglobin weist paramagnetische Eigenschaften auf und präsentiert daher in 7T T2*-gewichteten Sequenzen und in der suszeptibilitätsgewichteten MRT-Bildgebung einen Signalverlust. Dagegen ist oxygeniertes Hämoglobin diamagnetisch. Die Untersuchung der periventrikulären vaskulären Fläche der Patienten mit NMOSD zeigte im Vergleich zu HC nicht signifikant veränderte Werte. Es lässt sich daher vermuten, dass der Oxygenierungsgrad und/oder die Struktur der periventrikulären Venen von Patienten mit NMOSD denen von HC gleicht und somit nicht pathologisch verändert ist. Im Gegensatz dazu lassen sich bei Patienten mit MS weniger Venen im periventrikulären Raum in den T2*-gewichteten Aufnahmen (im Vergleich zu HC) darstellen. Dieses Ergebnis grenzt die NMOSD von der MS ab und weist auf einen Unterschied im Pathomechanismus dieser beiden Erkrankungen hin [28].

Die Ursache für eine reduzierte Sichtbarkeit venöser Strukturen bei MS-Betroffenen ist nicht abschließend geklärt. Eine Erklärung wäre ein zerebraler Hypometabolismus mit einer entsprechend reduzierten Sauerstoffausbeute: Der aus dem Hypometabolismus resultierende Verbleib von Sauerstoff im venösen Blut führt zu weniger desoxygeniertem Hämoglobin in den Venen bei MS-Patienten und damit zu einem geringeren Signalverlust in der T2*-gewichteten Bildgebung [28, 29].

In der Tat zeigte eine quantitative MRT-Studie von Ge et. al., dass Patienten mit MS im Vergleich zu Kontrollen eine durchschnittlich gesenkten Sauerstoffverbrauch bei gleichzeitig erhöhtem Sauerstoffgehalt des venösen Blutes haben [70]. Ebenso scheint es bei MS durch die vorherrschende Inflammation und Gliose [71] auch zu Schäden der Gefäße zu kommen, sodass es zur einer reduzierten zerebralen Perfusion [72] insgesamt kommt. Bei geringerer Perfusion ist die Sichtbarkeit der Venen in der T2*-gewichteten Bildgebung ebenfalls verschlechtert [28, 29]. Ein weiterer Grund einer geringeren Sauerstoffausschöpfung in den zerebralen Gefäßen von MS-Patienten scheint eine hohe Konzentration an Stickstoffmonoxid zu sein. Dieser wird bei wiederholten vaskulären Entzündungsreaktionen vermehrt freigesetzt und geht mit einer Hemmung der Sauerstoffaufnahme in den Mitochondrien einher [70].

Unsere Ergebnisse deuten darauf hin, dass die PVA bei NMOSD-Patienten im Gegensatz zu Patienten mit MS nicht reduziert ist. Es stellt sich die Frage, warum es bei MS-Patienten zu reduzierten PVA-Werten kommt, denn schließlich handelt es sich bei NMOSD und MS um entzündliche ZNS-Erkrankungen, die häufig zu schweren Behinderungen der Betroffenen führen. Eine Hypothese wäre, dass es bei der NMOSD eher zu fokalen Schäden und nur untergeordnet zu global-neurodegenerativen Prozessen kommt. Bisherige Erkenntnisse hierzu zeigen unterschiedliche Ergebnisse: Mittels Volumetrie wurde bei NMOSD vor allem eine Atrophie des Rückenmarks und eher eine geringe Ausprägung der Gehirnatrophie im Vergleich zu MS gesehen [73]. Die Arbeitsgruppe um Aboul-Enein et.al. sah via Spektroskopie keine signifikanten Unterschiede der normal erscheinenden weißen Hirnsubstanz von NMOSD und Kontrollen [74]. Ebenso wurden Veränderungen des Rückenmarks, der Sehstrahlung und des kortiko-spinalen Trakts in der Diffusions-Tensor-Bildgebung bei Patienten mit NMOSD im Vergleich zu Kontrollen gesehen [75]. Dem gegenüber zeigten von Glehn et.al. mittels Voxel-basierter Morphometrie bei NMOSD, dass es zu atrophischen Veränderungen der grauen Substanz im Frontal-, Parietal-, Temporal-, Okzipitallappen und des limbischen Systems kommt. Darüber hinaus zeigte sich eine Volumenreduktion der weißen Substanz zusätzlich im Hirnstamm, Kleinhirn, Chiasma opticum [76].

Neben Unterschieden im venösen System stellt sich ferner die Frage, ob es auch Unterschiede in der Läsionsmorphologie zwischen NMOSD und MS gibt. Hierzu durchgeführte 7T-MRT-Studien

konnten zeigen, dass innerhalb der zerebralen Läsionen kleine, zentrale Venen überzufällig bei Patienten mit MS anzufinden [25, 57, 77-82] und somit als mögliches Diagnosekriterium und zur Abgrenzung von anderen Erkrankungen einsetzbar sind [25, 26, 81, 83, 84].

Unter Verwendung hoher Feldstärken (7T) wird ebenso eine detaillierte Darstellung der magnetischen Mikroarchitektur von Läsionen des Zerebrums ermöglicht. Das im Rahmen der Magnetresonanz-Bildgebung in der Empfangsspule detektierte Signal lässt sich durch Frequenz, Amplitude und Phase beschreiben. Die Phase entspricht definitionsgemäß dem Schwingungszustand. Bei der Durchführung konventioneller MRT-Sequenzen wird vorwiegend die Amplitude zur Bildrekonstruktion als Korrelat der Signalintensität verwendet. Die Analyse von Veränderungen der Phase können zusätzlich Informationen erbringen, da das Vorhandensein paramagnetischer Substanzen zu positiven Phasenverschiebungen führt. Es ist möglich, diese Veränderungen in der Phase örtlich zuzuordnen und somit als Bild, bzw. „Map“, darzustellen. Wir haben diese Phasen-Maps genutzt, um Hirnläsionen genauer zu charakterisieren. Interessanterweise waren NMOSD-Läsionen auf Phasen-Maps gewöhnlich nicht vom umliegenden Hirngewebe zu unterscheiden, eine Phasenverschiebung hat somit nicht stattgefunden. Im Gegensatz hierzu waren MS-Läsionen oftmals auf diesen Phasen-Maps eindeutig abgrenzbar - entweder im Sinne ringförmiger oder nodulärer Strukturen. Dies entsprach jeweils einer positiven Phasenverschiebung. Was die Ursache dieser Phasenverschiebung innerhalb der SWI ist, ist Gegenstand aktueller Diskussionen. Diskutiert werden das Vorkommen eisenhaltiger Makrophagen oder Mikroglia [85], Proteine, Antikörper, Zytokine oder Zellen des Immunsystems als Ursache für eine ringförmige Phasenverschiebung um Läsionen von MS-Patienten [86]. Im Gegensatz dazu seien zentrale Phasenverschiebungen innerhalb der MS-Läsionen ein Hinweis auf Eisenablagerungen, die vermutlich aus dem Zugrundegehen von eisenhaltigen Oligodendrozyten [87], einem perivaskulären Hämoglobin-Leck [88] oder aus einem Verlust an diamagnetischen Myelin [89] resultieren. Die Abwesenheit solcher Phasenverschiebungen in Läsionen von NMOSD-Patienten deutet auf eine verschiedenartige Entstehung und anderen strukturellen Merkmalen bei NMOSD gegenüber MS-Läsionen hin [90].

Eine Gemeinsamkeit der hier untersuchten Erkrankungen ist die klinische Manifestation von zum Teil rezidivierenden ON, wodurch ein Augenmerk auch auf die Erhebung visueller Parameter lag. Der Vergleich von mittels OCT erhobenen pRNFL von Patienten mit MOG-Ak-assoziierter Enzephalomyelitis und AQP-4-Ak-positiver NMOSD ließen eine gleichermaßen stark ausgeprägte Ausdünnung dieser Schicht in beiden Gruppen erkennen. Auffällig war eine im Durchschnitt höhere ON-Schubrate in der Gruppe der Patienten mit MOG-Ak, wohingegen die Schäden der pRNFL bei AQP-4-Ak positiven Patienten eher durch weniger und dafür schwerwiegendere ON-Episoden verursacht wurden. Die Veränderungen der pRNFL nach durchgemachter ON von

MOG-Ak-positiven Patienten mit einem schubförmig-remittierenden Krankheitsverlauf untersuchten auch andere Studien [41, 42] über einen längeren Zeitraum (im Durchschnitt ~ 7 Jahre). Ihre Ergebnisse glichen unseren und zeigten eine gleichermaßen verdünnte pRNFL bei Patienten mit Nachweis von MOG-Ak und AQP-4-Ak. Hinsichtlich des neuro-axonalen Schaden der Retina zeigte zuletzt eine Studie von Akaishi et. al., dass der Verlust an retinalen Nervenfasern und der Schaden der Ganglionzellschicht bei 19 untersuchten MOG-Ak-positiven Patienten geringer war, als bei Patienten mit positivem Nachweis für AQP-4-Ak [49]. Die dabei untersuchten MOG-Ak-positiven Patienten wiesen jedoch, im Kontrast zu unserer Kohorte, alle einen monophasischen Krankheitsverlauf auf. Neueste Erkenntnisse der Arbeitsgruppe um Havla et. al weisen darauf hin, dass es bereits bei nicht ON-betroffenen Augen von Patienten mit positiven MOG-Ak-Nachweis zu einer signifikanten Reduktion der pRNFL vor allem der temporalen Quadranten kommt [91].
Betrachtet man das Auftreten von Schüben innerhalb des Krankheitsverlaufs, zeigen unsere, als auch die Ergebnisse anderer Arbeiten [92, 93], dass Patienten mit MOG-Antikörpernachweis häufig einen schubförmigen Verlauf präsentieren. Konträre Auswertungen weisen auf das Vorkommen monophasischer Verläufe mit einem insgesamt milden klinischen Phänotyp und schneller Rückbildung der Symptomatik bei MOG-Ak-positiven Patienten hin [3, 40, 94].

Zusammenfassung:

Durch die heutzutage zur Verfügung stehenden hochqualitativen diagnostischen Möglichkeiten, wie das UHF-MRT und das OCT, ist es uns möglich, pathophysiologische bedingte Unterschiede für die Abgrenzung neuroinflammatorischer Erkrankungen bereits *in vivo* festzustellen. Die in dieser Arbeit dargestellten Ergebnisse zeigen, dass sich die NMOSD von der MS durch nicht signifikant erniedrigte Werte der periventrikulären Venendichte, als auch durch überwiegend fehlende zentrale oder ringförmige Phasenverschiebungen in der Gradienten-Echo-basierten-Bildgebung abgrenzen. Weiterhin ermöglichen visuelle Untersuchungen die Differenzierung innerhalb der NMOSD-verwandten Erkrankungen selbst. Dabei weisen Patienten mit AQP-4-Ak zwar insgesamt ähnlich reduzierte Werte der pRNFL im OCT auf wie die MOG-Ak-positiven Patienten, dennoch zeigen sie im Durchschnitt eine geringere Schubanzahl bei tendenziell kürzeren, aber schwerwiegenderen Verläufen von ON. Dies geht mit einem größeren initialen Verlust der pRNFL bei ON-Erstereignis, als auch mit einem größeren Verlust des Sehvermögens der AQP-4-Ak-positiven Patienten einher. Die Zusammenschau aller hier erhaltenen Erkenntnisse erlaubt den Rückschluss, dass sich die NMOSD zum einen innerhalb ihrer verschiedenen Ausprägungen (AQP-4-Ak und MOG-Ak) und zum anderen in Abgrenzung zur MS hinsichtlich ihrer Pathomechanismen

unterscheiden. Im klinischen Alltag ist dieses Verständnis zur differentialdiagnostischen Abgrenzung von entscheidender Bedeutung.

1.7 Literaturverzeichnis

[1] D.M. Wingerchuk, B. Banwell, J.L. Bennett, P. Cabre, W. Carroll, T. Chitnis, J. de Seze, K. Fujihara, B. Greenberg, A. Jacob, S. Jarius, M. Lana-Peixoto, M. Levy, J.H. Simon, S. Tenembaum, A.L. Traboulsee, P. Waters, K.E. Wellik, B.G. Weinshenker, International consensus diagnostic criteria for neuromyelitis optica spectrum disorders, Neurology, (2015).

[2] V.A. Lennon, D.M. Wingerchuk, T.J. Kryzer, S.J. Pittock, C.F. Lucchinetti, K. Fujihara, I. Nakashima, B.G. Weinshenker, A serum autoantibody marker of neuromyelitis optica: distinction from multiple sclerosis, Lancet, 364 (2004) 2106-2112.

[3] S. Jarius, K. Ruprecht, B. Wildemann, T. Kuempfel, M. Ringelstein, C. Geis, I. Kleiter, C. Kleinschnitz, A. Berthele, J. Brettschneider, K. Hellwig, B. Hemmer, R.A. Linker, F. Lauda, C.A. Mayer, H. Tumani, A. Melms, C. Trebst, M. Stangel, M. Marziniak, F. Hoffmann, S. Schippling, J.H. Faiss, O. Neuhaus, B. Ettrich, C. Zentner, K. Guthke, U. Hofstadt-van Oy, R. Reuss, H. Pellkofer, U. Ziemann, P. Kern, K.P. Wandinger, F.T. Bergh, T. Boettcher, S. Langel, M. Liebetrau, P.S. Rommer, S. Niehaus, C. Münch, A. Winkelmann, U.K. Zettl U, I. Metz, C. Veauthier, J.P. Sieb, C. Wilke, H.P. Hartung, O. Aktas, F. Paul, Contrasting disease patterns in seropositive and seronegative neuromyelitis optica: A multicentre study of 175 patients, J Neuroinflammation, 9 (2012) 14.

[4] C. Trebst, S. Jarius, A. Berthele, F. Paul, S. Schippling, B. Wildemann, N. Borisow, I. Kleiter, O. Aktas, T. Kümpfel, N.O.S.G. (NEMOS), Update on the diagnosis and treatment of neuromyelitis optica: recommendations of the Neuromyelitis Optica Study Group (NEMOS), J Neurol, 261 (2014) 1-16.

[5] S. Jarius, B. Wildemann, F. Paul, Neuromyelitis optica: clinical features, immunopathogenesis, and treatment, Clin Exp Immunol, (2014).

[6] I. Metz, T. Beißbarth, D. Ellenberger, F. Pache, L. Stork, M. Ringelstein, O. Aktas, S. Jarius, B. Wildemann, H. Dihazi, T. Friede, W. Brück, K. Ruprecht, F. Paul, Serum peptide reactivities may distinguish neuromyelitis optica subgroups and multiple sclerosis, Neurol Neuroimmunol Neuroinflamm, 3 (2016) e204.

[7] V.S. Chavarro, M.A. Mealy, A. Simpson, A. Lacheta, F. Pache, K. Ruprecht, S.M. Gold, F. Paul, A.U. Brandt, M. Levy, Insufficient treatment of severe depression in neuromyelitis optica spectrum disorder, Neurol Neuroimmunol Neuroinflamm, 3 (2016) e286.

[8] L. Pandit, N. Asgari, M. Apiwattanakul, J. Palace, F. Paul, M.I. Leite, I. Kleiter, T. Chitnis, G.I.C.C.B.f.N. Optica, Demographic and clinical features of neuromyelitis optica: A review, Mult Scler, 21 (2015) 845-853.

[9] H.J. Kim, F. Paul, M.A. Lana-Peixoto, S. Tenembaum, N. Asgari, J. Palace, E.C. Klawiter, D.K. Sato, J. de Seze, J. Wuerfel, B.L. Banwell, P. Villoslada, A. Saiz, K. Fujihara, S.H. Kim, G.-J.C.F.N.I.C.C. Biorepository, MRI characteristics of neuromyelitis optica spectrum disorder: an international update, Neurology, 84 (2015) 1165-1173.

[10] N. Borisow, I. Kleiter, A. Gahlen, K. Fischer, K.D. Wernecke, F. Pache, K. Ruprecht, J. Havla, M. Krumbholz, T. Kümpfel, O. Aktas, M. Ringelstein, C. Geis, C. Kleinschnitz, A. Berthele, B. Hemmer, K. Angstwurm, R. Weissert, J.P. Stellmann, S. Schuster, M. Stangel, F. Lauda, H. Tumani, C. Mayer, L. Zeltner, U. Ziemann, R.A. Linker, M. Schwab, M. Marziniak, F. Then Bergh, U. Hofstadt-van Oy, O. Neuhaus, A. Winkelmann, W. Marouf, L. Rückriem, J. Faiss, B. Wildemann, F. Paul, S. Jarius, C. Trebst, K. Hellwig, N.N.O.S. Group), Influence of female sex and fertile age on neuromyelitis optica spectrum disorders, Mult Scler, 23 (2017) 1092-1103.

[11] N. Asgari, E.P. Flanagan, K. Fujihara, H.J. Kim, H.P. Skejoe, J. Wuerfel, H. Kuroda, S.H. Kim, E. Maillart, R. Marignier, S.J. Pittock, F. Paul, B.G. Weinshenker, Disruption of the leptomeningeal blood barrier in neuromyelitis optica spectrum disorder, Neurol Neuroimmunol Neuroinflamm, 4 (2017) e343.

[12] D. Whittam, M. Bhojak, K. Das, A. Jacob, Longitudinally extensive myelitis in MS mimicking neuromyelitis optica, Neurol Neuroimmunol Neuroinflamm, 4 (2017) e333.

[13] C. Finke, J. Heine, F. Pache, A. Lacheta, N. Borisow, J. Kuchling, J. Bellmann-Strobl, K. Ruprecht, A.U. Brandt, F. Paul, Normal volumes and microstructural integrity of deep gray matter structures in AQP4+ NMOSD, Neurol Neuroimmunol Neuroinflamm, 3 (2016) e229.

[14] Y. Takeshita, B. Obermeier, A.C. Cotleur, S.F. Spampinato, F. Shimizu, E. Yamamoto, Y. Sano, T.J. Kryzer, V.A. Lennon, T. Kanda, R.M. Ransohoff, Effects of neuromyelitis optica-IgG at the blood-brain barrier in vitro, Neurol Neuroimmunol Neuroinflamm, 4 (2017) e311.

[15] V. Davoudi, K. Keyhanian, R.M. Bove, T. Chitnis, Immunology of neuromyelitis optica during pregnancy, Neurol Neuroimmunol Neuroinflamm, 3 (2016) e288.

[16] F. Pache, B. Wildemann, F. Paul, S. Jarius, [Neuromyelitis optica], Fortschr Neurol Psychiatr, 85 (2017) 100-114.

[17] L. Hertwig, F. Pache, S. Romero-Suarez, K.H. Stürner, N. Borisow, J. Behrens, J. Bellmann-Strobl, B. Seeger, N. Asselborn, K. Ruprecht, J.M. Millward, C. Infante-Duarte, F. Paul, Distinct functionality of neutrophils in multiple sclerosis and neuromyelitis optica, Mult Scler, 22 (2016) 160-173.

[18] J.P. Stellmann, M. Krumbholz, T. Friede, A. Gahlen, N. Borisow, K. Fischer, K. Hellwig, F. Pache, K. Ruprecht, J. Havla, T. Kümpfel, O. Aktas, H.P. Hartung, M. Ringelstein, C. Geis, C. Kleinschnitz, A. Berthele, B. Hemmer, K. Angstwurm, K.L. Young, S. Schuster, M. Stangel, F.

Lauda, H. Tumani, C. Mayer, L. Zeltner, U. Ziemann, R.A. Linker, M. Schwab, M. Marziniak, F. Then Bergh, U. Hofstadt-van Oy, O. Neuhaus, U. Zettl, J. Faiss, B. Wildemann, F. Paul, S. Jarius, C. Trebst, I. Kleiter, N.N.O.S. Group), Immunotherapies in neuromyelitis optica spectrum disorder: efficacy and predictors of response, J Neurol Neurosurg Psychiatry, 88 (2017) 639-647.

[19] I. Ayzenberg, J. Schöllhammer, R. Hoepner, K. Hellwig, M. Ringelstein, O. Aktas, T. Kümpfel, M. Krumbholz, C. Trebst, F. Paul, F. Pache, M. Obermann, L. Zeltner, M. Schwab, A. Berthele, S. Jarius, I. Kleiter, N.O.S. Group, Efficacy of glatiramer acetate in neuromyelitis optica spectrum disorder: a multicenter retrospective study, J Neurol, 263 (2016) 575-582.

[20] I. Kleiter, A. Gahlen, N. Borisow, K. Fischer, K.D. Wernecke, B. Wegner, K. Hellwig, F. Pache, K. Ruprecht, J. Havla, M. Krumbholz, T. Kümpfel, O. Aktas, H.P. Hartung, M. Ringelstein, C. Geis, C. Kleinschnitz, A. Berthele, B. Hemmer, K. Angstwurm, J.P. Stellmann, S. Schuster, M. Stangel, F. Lauda, H. Tumani, C. Mayer, L. Zeltner, U. Ziemann, R. Linker, M. Schwab, M. Marziniak, F. Then Bergh, U. Hofstadt-van Oy, O. Neuhaus, A. Winkelmann, W. Marouf, J. Faiss, B. Wildemann, F. Paul, S. Jarius, C. Trebst, N.O.S. Group, Neuromyelitis optica: Evaluation of 871 attacks and 1,153 treatment courses, Ann Neurol, 79 (2016) 206-216.

[21] P. Valentino, F. Marnetto, L. Granieri, M. Capobianco, A. Bertolotto, Aquaporin-4 antibody titration in NMO patients treated with rituximab: A retrospective study, Neurol Neuroimmunol Neuroinflamm, 4 (2017) e317.

[22] I. Kleiter, K. Hellwig, A. Berthele, T. Kümpfel, R.A. Linker, H.P. Hartung, F. Paul, O. Aktas, N.O.S. Group, Failure of natalizumab to prevent relapses in neuromyelitis optica, Arch Neurol, 69 (2012) 239-245.

[23] A. Gahlen, A.K. Trampe, S. Haupeltshofer, M. Ringelstein, O. Aktas, A. Berthele, B. Wildemann, R. Gold, S. Jarius, I. Kleiter, Aquaporin-4 antibodies in patients treated with natalizumab for suspected MS, Neurol Neuroimmunol Neuroinflamm, 4 (2017) e363.

[24] T. Sinnecker, J. Kuchling, P. Dusek, J. Dörr, T. Niendorf, F. Paul, J. Wuerfel, Ultrahigh field MRI in clinical neuroimmunology: a potential contribution to improved diagnostics and personalised disease management, EPMA J, 6 (2015) 16.

[25] T. Sinnecker, J. Dörr, C.F. Pfueller, L. Harms, K. Ruprecht, S. Jarius, W. Brück, T. Niendorf, J. Wuerfel, F. Paul, Distinct lesion morphology at 7-T MRI differentiates neuromyelitis optica from multiple sclerosis, Neurology, 79 (2012) 708-714.

[26] I. Kister, J. Herbert, Y. Zhou, Y. Ge, Ultrahigh-Field MR (7 T) Imaging of Brain Lesions in Neuromyelitis Optica, Mult Scler Int, 2013 (2013) 398259.

[27] T. Sinnecker, P. Mittelstaedt, J. Dörr, C.F. Pfueller, L. Harms, T. Niendorf, F. Paul, J. Wuerfel, Multiple sclerosis lesions and irreversible brain tissue damage: a comparative ultrahigh-field strength magnetic resonance imaging study, Arch Neurol, 69 (2012) 739-745.

[28] T. Sinnecker, I. Bozin, J. Dörr, C.F. Pfueller, L. Harms, T. Niendorf, A.U. Brandt, F. Paul, J. Wuerfel, Periventricular venous density in multiple sclerosis is inversely associated with T2 lesion count: a 7 Tesla MRI study, Mult Scler, 19 (2013) 316-325.

[29] Y. Ge, V.M. Zohrabian, E.O. Osa, J. Xu, H. Jaggi, J. Herbert, E.M. Haacke, R.I. Grossman, Diminished visibility of cerebral venous vasculature in multiple sclerosis by susceptibility-weighted imaging at 3.0 Tesla, J Magn Reson Imaging, 29 (2009) 1190-1194.

[30] S. Jarius, K. Ruprecht, I. Kleiter, N. Borisow, N. Asgari, K. Pitarokoili, F. Pache, O. Stich, L.A. Beume, M.W. Hümmert, M. Ringelstein, C. Trebst, A. Winkelmann, A. Schwarz, M. Buttmann, H. Zimmermann, J. Kuchling, D. Franciotta, M. Capobianco, E. Siebert, C. Lukas, M. Korporal-Kuhnke, J. Haas, K. Fechner, A.U. Brandt, K. Schanda, O. Aktas, F. Paul, M. Reindl, B. Wildemann, i.c.w.t.N.O.S.G. (NEMOS), MOG-IgG in NMO and related disorders: a multicenter study of 50 patients. Part 2: Epidemiology, clinical presentation, radiological and laboratory features, treatment responses, and long-term outcome, J Neuroinflammation, 13 (2016) 280.

[31] S. Jarius, K. Ruprecht, I. Kleiter, N. Borisow, N. Asgari, K. Pitarokoili, F. Pache, O. Stich, L.A. Beume, M.W. Hümmert, C. Trebst, M. Ringelstein, O. Aktas, A. Winkelmann, M. Buttmann, A. Schwarz, H. Zimmermann, A.U. Brandt, D. Franciotta, M. Capobianco, J. Kuchling, J. Haas, M. Korporal-Kuhnke, S.T. Lillevang, K. Fechner, K. Schanda, F. Paul, B. Wildemann, M. Reindl, i.c.w.t.N.O.S.G. (NEMOS), MOG-IgG in NMO and related disorders: a multicenter study of 50 patients. Part 1: Frequency, syndrome specificity, influence of disease activity, long-term course, association with AQP4-IgG, and origin, J Neuroinflammation, 13 (2016) 279.

[32] S. Jarius, I. Kleiter, K. Ruprecht, N. Asgari, K. Pitarokoili, N. Borisow, M.W. Hümmert, C. Trebst, F. Pache, A. Winkelmann, L.A. Beume, M. Ringelstein, O. Stich, O. Aktas, M. Korporal-Kuhnke, A. Schwarz, C. Lukas, J. Haas, K. Fechner, M. Buttmann, J. Bellmann-Strobl, H. Zimmermann, A.U. Brandt, D. Franciotta, K. Schanda, F. Paul, M. Reindl, B. Wildemann, i.c.w.t.N.O.S.G. (NEMOS), MOG-IgG in NMO and related disorders: a multicenter study of 50 patients. Part 3: Brainstem involvement - frequency, presentation and outcome, J Neuroinflammation, 13 (2016) 281.

[33] P. Körtvélyessy, M. Breu, M. Pawlitzki, I. Metz, H.J. Heinze, M. Matzke, C. Mawrin, P. Rommer, G.G. Kovacs, C. Mitter, M. Reindl, W. Brück, K.P. Wandinger, H. Lassmann, R. Höftberger, F. Leypoldt, ADEM-like presentation, anti-MOG antibodies, and MS pathology: TWO case reports, Neurol Neuroimmunol Neuroinflamm, 4 (2017) e335.

[34] R. Ogawa, I. Nakashima, T. Takahashi, K. Kaneko, T. Akaishi, Y. Takai, D.K. Sato, S. Nishiyama, T. Misu, H. Kuroda, M. Aoki, K. Fujihara, MOG antibody-positive, benign, unilateral, cerebral cortical encephalitis with epilepsy, Neurol Neuroimmunol Neuroinflamm, 4 (2017) e322.
[35] M. Spadaro, L.A. Gerdes, M. Krumbholz, B. Ertl-Wagner, F.S. Thaler, E. Schuh, I. Metz, A. Blaschek, A. Dick, W. Brück, R. Hohlfeld, E. Meinl, T. Kümpfel, Autoantibodies to MOG in a distinct subgroup of adult multiple sclerosis, Neurol Neuroimmunol Neuroinflamm, 3 (2016) e257.
[36] M. Sepúlveda, T. Armangué, N. Sola-Valls, G. Arrambide, J.E. Meca-Lallana, C. Oreja-Guevara, M. Mendibe, A. Alvarez de Arcaya, Y. Aladro, B. Casanova, J. Olascoaga, A. Jiménez-Huete, M. Fernández-Fournier, L. Ramió-Torrentà, A. Cobo-Calvo, M. Viñals, C. de Andrés, V. Meca-Lallana, A. Cervelló, C. Calles, M.B. Rubio, C. Ramo-Tello, A. Caminero, E. Munteis, A.R. Antigüedad, Y. Blanco, P. Villoslada, X. Montalban, F. Graus, A. Saiz, Neuromyelitis optica spectrum disorders: Comparison according to the phenotype and serostatus, Neurol Neuroimmunol Neuroinflamm, 3 (2016) e225.
[37] O. Aktas, Collateral benefit: the comeback of MOG antibodies as a biomarker in neurological practice, J Neurol Neurosurg Psychiatry, 86 (2015) 243.
[38] M. Reindl, K. Rostasy, MOG antibody-associated diseases, Neurol Neuroimmunol Neuroinflamm, 2 (2015) e60.
[39] S.S. Zamvil, A.J. Slavin, Does MOG Ig-positive AQP4-seronegative opticospinal inflammatory disease justify a diagnosis of NMO spectrum disorder?, Neurol Neuroimmunol Neuroinflamm, 2 (2015) e62.
[40] D.K. Sato, D. Callegaro, M.A. Lana-Peixoto, P.J. Waters, F.M. de Haidar Jorge, T. Takahashi, I. Nakashima, S.L. Apostolos-Pereira, N. Talim, R.F. Simm, A.M. Lino, T. Misu, M.I. Leite, M. Aoki, K. Fujihara, Distinction between MOG antibody-positive and AQP4 antibody-positive NMO spectrum disorders, Neurology, 82 (2014) 474-481.
[41] J.L. Bennett, J. de Seze, M. Lana-Peixoto, J. Palace, A. Waldman, S. Schippling, S. Tenembaum, B. Banwell, B. Greenberg, M. Levy, K. Fujihara, K.H. Chan, H.J. Kim, N. Asgari, D.K. Sato, A. Saiz, J. Wuerfel, H. Zimmermann, A. Green, P. Villoslada, F. Paul, GJCF-ICC&BR, Neuromyelitis optica and multiple sclerosis: Seeing differences through optical coherence tomography, Mult Scler, 21 (2015) 678-688.
[42] E. Schneider, H. Zimmermann, T. Oberwahrenbrock, F. Kaufhold, E.M. Kadas, A. Petzold, F. Bilger, N. Borisow, S. Jarius, B. Wildemann, K. Ruprecht, A.U. Brandt, F. Paul, Optical Coherence Tomography Reveals Distinct Patterns of Retinal Damage in Neuromyelitis Optica and Multiple Sclerosis, PLoS One, 8 (2013) e66151.

[43] F.C. Oertel, J. Kuchling, H. Zimmermann, C. Chien, F. Schmidt, B. Knier, J. Bellmann-Strobl, T. Korn, M. Scheel, A. Klistorner, K. Ruprecht, F. Paul, A.U. Brandt, Microstructural visual system changes in AQP4-antibody-seropositive NMOSD, Neurol Neuroimmunol Neuroinflamm, 4 (2017) e334.

[44] F.C. Oertel, H. Zimmermann, J. Mikolajczak, M. Weinhold, E.M. Kadas, T. Oberwahrenbrock, F. Pache, J. Bellmann-Strobl, K. Ruprecht, F. Paul, A.U. Brandt, Contribution of blood vessels to retinal nerve fiber layer thickness in NMOSD, Neurol Neuroimmunol Neuroinflamm, 4 (2017) e338.

[45] F. Schmidt, H. Zimmermann, J. Mikolajczak, F.C. Oertel, F. Pache, M. Weinhold, J. Schinzel, J. Bellmann-Strobl, K. Ruprecht, F. Paul, A.U. Brandt, Severe structural and functional visual system damage leads to profound loss of vision-related quality of life in patients with neuromyelitis optica spectrum disorders, Mult Scler Relat Disord, 11 (2017) 45-50.

[46] F. Kaufhold, H. Zimmermann, E. Schneider, K. Ruprecht, F. Paul, T. Oberwahrenbrock, A.U. Brandt, Optic neuritis is associated with inner nuclear layer thickening and microcystic macular edema independently of multiple sclerosis, PLoS One, 8 (2013) e71145.

[47] E.S. Sotirchos, S. Saidha, G. Byraiah, M.A. Mealy, M.A. Ibrahim, Y.J. Sepah, S.D. Newsome, J.N. Ratchford, E.M. Frohman, L.J. Balcer, C.M. Crainiceanu, Q.D. Nguyen, M. Levy, P.A. Calabresi, In vivo identification of morphologic retinal abnormalities in neuromyelitis optica, Neurology, 80 (2013) 1406-1414.

[48] A.U. Brandt, T. Oberwahrenbrock, E.M. Kadas, W.A. Lagrèze, F. Paul, Dynamic formation of macular microcysts independent of vitreous traction changes, Neurology, 83 (2014) 73-77.

[49] T. Akaishi, D.K. Sato, I. Nakashima, T. Takeshita, T. Takahashi, H. Doi, K. Kurosawa, K. Kaneko, H. Kuroda, S. Nishiyama, T. Misu, T. Nakazawa, K. Fujihara, M. Aoki, MRI and retinal abnormalities in isolated optic neuritis with myelin oligodendrocyte glycoprotein and aquaporin-4 antibodies: a comparative study, J Neurol Neurosurg Psychiatry, 87 (2016) 446-448.

[50] E. Martinez-Hernandez, M. Sepulveda, K. Rostásy, R. Höftberger, F. Graus, R.J. Harvey, A. Saiz, J. Dalmau, Antibodies to aquaporin 4, myelin-oligodendrocyte glycoprotein, and the glycine receptor α1 subunit in patients with isolated optic neuritis, JAMA Neurol, 72 (2015) 187-193.

[51] S. Schumacher, F. Pache, J. Bellmann-Strobl, J. Behrens, P. Dusek, L. Harms, K. Ruprecht, P. Nytrova, S. Chawla, T. Niendorf, I. Kister, F. Paul, Y. Ge, J. Wuerfel, T. Sinnecker, Neuromyelitis optica does not impact periventricular venous density versus healthy controls: a 7.0 Tesla MRI clinical study, MAGMA, 29 (2016) 535-541.

[52] T. Sinnecker, S. Schumacher, K. Mueller, F. Pache, P. Dusek, L. Harms, K. Ruprecht, P. Nytrova, S. Chawla, T. Niendorf, I. Kister, F. Paul, Y. Ge, J. Wuerfel, MRI phase changes in

multiple sclerosis vs neuromyelitis optica lesions at 7T, Neurol Neuroimmunol Neuroinflamm, 3 (2016) e259.

[53] F. Pache, H. Zimmermann, J. Mikolajczak, S. Schumacher, A. Lacheta, F.C. Oertel, J. Bellmann-Strobl, S. Jarius, B. Wildemann, M. Reindl, A. Waldman, K. Soelberg, N. Asgari, M. Ringelstein, O. Aktas, N. Gross, M. Buttmann, T. Ach, K. Ruprecht, F. Paul, A.U. Brandt, i.c.w.t.N.O.S.G. (NEMOS), MOG-IgG in NMO and related disorders: a multicenter study of 50 patients. Part 4: Afferent visual system damage after optic neuritis in MOG-IgG-seropositive versus AQP4-IgG-seropositive patients, J Neuroinflammation, 13 (2016) 282.

[54] A. Rosset, L. Spadola, O. Ratib, OsiriX: an open-source software for navigating in multidimensional DICOM images, J Digit Imaging, 17 (2004) 205-216.

[55] R. Emmerson-Hanover, D.E. Shearer, D.J. Creel, R.E. Dustman, Pattern reversal evoked potentials: gender differences and age-related changes in amplitude and latency, Electroencephalogr Clin Neurophysiol, 92 (1994) 93-101.

[56] The R Project for Statistical Computing, in: N.S.o.E. Roger Bivand, Bergen, Norway (Ed.), Simon Urbanek & Martyn Plummer.

[57] J. Kuchling, T. Sinnecker, I. Bozin, J. Dörr, V.I. Madai, J. Sobesky, T. Niendorf, F. Paul, J. Wuerfel, [Ultrahigh field MRI in context of neurological diseases], Nervenarzt, 85 (2014) 445-458.

[58] T. Sinnecker, J. Othman, M. Kühl, R. Mekle, I. Selbig, T. Niendorf, A. Kunkel, P. Wienecke, P. Kern, F. Paul, J. Faiss, J. Wuerfel, 7T MRI in natalizumab-associated PML and ongoing MS disease activity: A case study, Neurol Neuroimmunol Neuroinflamm, 2 (2015) e171.

[59] T. Sinnecker, T. Oberwahrenbrock, I. Metz, H. Zimmermann, C.F. Pfueller, L. Harms, K. Ruprecht, C. Ramien, K. Hahn, W. Brück, T. Niendorf, F. Paul, A.U. Brandt, J. Dörr, J. Wuerfel, Optic radiation damage in multiple sclerosis is associated with visual dysfunction and retinal thinning--an ultrahigh-field MR pilot study, Eur Radiol, 25 (2015) 122-131.

[60] M. Bock, F. Paul, J. Dörr, [Diagnosis and monitoring of multiple sclerosis: the value of optical coherence tomography], Nervenarzt, 84 (2013) 483-492.

[61] A.U. Brandt, Zimmermann, H., Scheel, M., Finke, C., Albrecht, P., Paul, F., Untersuchungen des visuellen Systems in der Neurologie: aktuelle Forschung und klinische Relevanz, Aktuelle Neurologie, (2017) 27-45.

[62] M. Ringelstein, I. Kleiter, I. Ayzenberg, N. Borisow, F. Paul, K. Ruprecht, M. Kraemer, E. Cohn, B. Wildemann, S. Jarius, H.P. Hartung, O. Aktas, P. Albrecht, Visual evoked potentials in neuromyelitis optica and its spectrum disorders, Mult Scler, 20 (2014) 617-620.

[63] S. Jarius, F. Paul, D. Franciotta, P. Waters, F. Zipp, R. Hohlfeld, A. Vincent, B. Wildemann, Mechanisms of disease: aquaporin-4 antibodies in neuromyelitis optica, Nat Clin Pract Neurol, 4 (2008) 202-214.

[64] F. Paul, S. Jarius, O. Aktas, M. Bluthner, O. Bauer, H. Appelhans, D. Franciotta, R. Bergamaschi, E. Littleton, J. Palace, H.P. Seelig, R. Hohlfeld, A. Vincent, F. Zipp, Antibody to aquaporin 4 in the diagnosis of neuromyelitis optica, PLoS Med, 4 (2007) e133.

[65] B. Wildemann, S. Jarius, F. Paul, [Neuromyelitis optica], Nervenarzt, 84 (2013) 436-441.

[66] A. Zekeridou, V.A. Lennon, Aquaporin-4 autoimmunity, Neurol Neuroimmunol Neuroinflamm, 2 (2015) e110.

[67] C. Trebst, A. Berthele, S. Jarius, T. Kümpfel, S. Schippling, B. Wildemann, C. Wilke, N.o.S. (NEMOS), [Diagnosis and treatment of neuromyelitis optica. Consensus recommendations of the Neuromyelitis Optica Study Group], Nervenarzt, 82 (2011) 768-777.

[68] A. Bar-Or, L. Steinman, J.M. Behne, D. Benitez-Ribas, P.S. Chin, M. Clare-Salzler, D. Healey, J.I. Kim, D.M. Kranz, A. Lutterotti, R. Martin, S. Schippling, P. Villoslada, C.H. Wei, H.L. Weiner, S.S. Zamvil, T.J. Smith, M.R. Yeaman, Restoring immune tolerance in neuromyelitis optica: Part II, Neurol Neuroimmunol Neuroinflamm, 3 (2016) e277.

[69] L. Steinman, A. Bar-Or, J.M. Behne, D. Benitez-Ribas, P.S. Chin, M. Clare-Salzler, D. Healey, J.I. Kim, D.M. Kranz, A. Lutterotti, R. Martin, S. Schippling, P. Villoslada, C.H. Wei, H.L. Weiner, S.S. Zamvil, M.R. Yeaman, T.J. Smith, Restoring immune tolerance in neuromyelitis optica: Part I, Neurol Neuroimmunol Neuroinflamm, 3 (2016) e276.

[70] Y. Ge, Z. Zhang, H. Lu, L. Tang, H. Jaggi, J. Herbert, J.S. Babb, H. Rusinek, R.I. Grossman, Characterizing brain oxygen metabolism in patients with multiple sclerosis with T2-relaxation-under-spin-tagging MRI, J Cereb Blood Flow Metab, 32 (2012) 403-412.

[71] C.W. Adams, Perivascular iron deposition and other vascular damage in multiple sclerosis, J Neurol Neurosurg Psychiatry, 51 (1988) 260-265.

[72] J. Wuerfel, F. Paul, F. Zipp, Cerebral blood perfusion changes in multiple sclerosis, J Neurol Sci, 259 (2007) 16-20.

[73] Y. Liu, J. Wang, M. Daams, F. Weiler, H.K. Hahn, Y. Duan, J. Huang, Z. Ren, J. Ye, H. Dong, H. Vrenken, M.P. Wattjes, F.D. Shi, K. Li, F. Barkhof, Differential patterns of spinal cord and brain atrophy in NMO and MS, Neurology, 84 (2015) 1465-1472.

[74] F. Aboul-Enein, M. Krssák, R. Höftberger, D. Prayer, W. Kristoferitsch, Diffuse white matter damage is absent in neuromyelitis optica, AJNR Am J Neuroradiol, 31 (2010) 76-79.

[75] J. Jeantroux, S. Kremer, X.Z. Lin, N. Collongues, J.B. Chanson, B. Bourre, M. Fleury, F. Blanc, J.L. Dietemann, J. de Seze, Diffusion tensor imaging of normal-appearing white matter in neuromyelitis optica, J Neuroradiol, 39 (2012) 295-300.

[76] F. von Glehn, S. Jarius, R.P. Cavalcanti Lira, M.C. Alves Ferreira, F.H. von Glehn, S.M. Costa E Castro, G.C. Beltramini, F.P. Bergo, A.S. Farias, C.O. Brandão, B. Wildemann, B.P. Damasceno, F. Cendes, L.M. Santos, C.L. Yasuda, Structural brain abnormalities are related to retinal nerve fiber layer thinning and disease duration in neuromyelitis optica spectrum disorders, Mult Scler, 20 (2014) 1189-1197.

[77] D. Pitt, A. Boster, W. Pei, E. Wohleb, A. Jasne, C.R. Zachariah, K. Rammohan, M.V. Knopp, P. Schmalbrock, Imaging cortical lesions in multiple sclerosis with ultra-high-field magnetic resonance imaging, Arch Neurol, 67 (2010) 812-818.

[78] Y. Ge, V.M. Zohrabian, R.I. Grossman, Seven-Tesla magnetic resonance imaging: new vision of microvascular abnormalities in multiple sclerosis, Arch Neurol, 65 (2008) 812-816.

[79] K. Kollia, S. Maderwald, N. Putzki, M. Schlamann, J.M. Theysohn, O. Kraff, M.E. Ladd, M. Forsting, I. Wanke, First clinical study on ultra-high-field MR imaging in patients with multiple sclerosis: comparison of 1.5T and 7T, AJNR Am J Neuroradiol, 30 (2009) 699-702.

[80] K. Müller, J. Kuchling, J. Dörr, L. Harms, K. Ruprecht, T. Niendorf, J. Wuerfel, F. Paul, T. Sinnecker, Detailing intra-lesional venous lumen shrinking in multiple sclerosis investigated by sFLAIR MRI at 7-T, J Neurol, 261 (2014) 2032-2036.

[81] J. Wuerfel, T. Sinnecker, E.B. Ringelstein, S. Jarius, W. Schwindt, T. Niendorf, F. Paul, I. Kleffner, J. Dörr, Lesion morphology at 7 Tesla MRI differentiates Susac syndrome from multiple sclerosis, Mult Scler, 18 (2012) 1592-1599.

[82] J. Kuchling, C. Ramien, I. Bozin, J. Dörr, L. Harms, B. Rosche, T. Niendorf, F. Paul, T. Sinnecker, J. Wuerfel, Identical lesion morphology in primary progressive and relapsing-remitting MS--an ultrahigh field MRI study, Mult Scler, 20 (2014) 1866-1871.

[83] I. Kister, Y. Ge, J. Herbert, T. Sinnecker, J. Wuerfel, F. Paul, Distinction of seropositive NMO spectrum disorder and MS brain lesion distribution, Neurology, 81 (2013) 1966.

[84] M. Blaabjerg, K. Ruprecht, T. Sinnecker, D. Kondziella, T. Niendorf, B.M. Kerrn-Jespersen, M. Lindelof, H. Lassmann, B.W. Kristensen, F. Paul, Z. Illes, Widespread inflammation in CLIPPERS syndrome indicated by autopsy and ultra-high-field 7T MRI, Neurol Neuroimmunol Neuroinflamm, 3 (2016) e226.

[85] E.P. Flanagan, B.G. Weinshenker, K.N. Krecke, V.A. Lennon, C.F. Lucchinetti, A. McKeon, D.M. Wingerchuk, E.A. Shuster, Y. Jiao, E.S. Horta, S.J. Pittock, Short Myelitis Lesions in Aquaporin-4-IgG-Positive Neuromyelitis Optica Spectrum Disorders, JAMA Neurol, (2014).

[86] M. Absinta, P. Sati, M.I. Gaitán, P. Maggi, I.C. Cortese, M. Filippi, D.S. Reich, Seven-tesla phase imaging of acute multiple sclerosis lesions: a new window into the inflammatory process, Ann Neurol, 74 (2013) 669-678.

[87] S. Hametner, I. Wimmer, L. Haider, S. Pfeifenbring, W. Brück, H. Lassmann, Iron and neurodegeneration in the multiple sclerosis brain, Ann Neurol, 74 (2013) 848-861.

[88] F. Bagnato, S. Hametner, B. Yao, P. van Gelderen, H. Merkle, F.K. Cantor, H. Lassmann, J.H. Duyn, Tracking iron in multiple sclerosis: a combined imaging and histopathological study at 7 Tesla, Brain, 134 (2011) 3602-3615.

[89] W. Li, B. Wu, C. Liu, Quantitative susceptibility mapping of human brain reflects spatial variation in tissue composition, Neuroimage, 55 (2011) 1645-1656.

[90] W. Brück, B. Popescu, C.F. Lucchinetti, S. Markovic-Plese, R. Gold, D.R. Thal, I. Metz, Neuromyelitis optica lesions may inform multiple sclerosis heterogeneity debate, Ann Neurol, 72 (2012) 385-394.

[91] J. Havla, T. Kümpfel, R. Schinner, M. Spadaro, E. Schuh, E. Meinl, R. Hohlfeld, O. Outteryck, Myelin-oligodendrocyte-glycoprotein (MOG) autoantibodies as potential markers of severe optic neuritis and subclinical retinal axonal degeneration, J Neurol, 264 (2017) 139-151.

[92] S. Ramanathan, S.W. Reddel, A. Henderson, J.D. Parratt, M. Barnett, P.N. Gatt, V. Merheb, R.Y. Kumaran, K. Pathmanandavel, N. Sinmaz, M. Ghadiri, C. Yiannikas, S. Vucic, G. Stewart, A.F. Bleasel, D. Booth, V.S. Fung, R.C. Dale, F. Brilot, Antibodies to myelin oligodendrocyte glycoprotein in bilateral and recurrent optic neuritis, Neurol Neuroimmunol Neuroinflamm, 1 (2014) e40.

[93] K. Chalmoukou, H. Alexopoulos, S. Akrivou, P. Stathopoulos, M. Reindl, M.C. Dalakas, Anti-MOG antibodies are frequently associated with steroid-sensitive recurrent optic neuritis, Neurol Neuroimmunol Neuroinflamm, 2 (2015) e131.

[94] J. Kitley, P. Waters, M. Woodhall, M.I. Leite, A. Murchison, J. George, W. Küker, S. Chandratre, A. Vincent, J. Palace, Neuromyelitis optica spectrum disorders with aquaporin-4 and myelin-oligodendrocyte glycoprotein antibodies: a comparative study, JAMA Neurol, 71 (2014) 276-283.

2. Eidesstattliche Versicherung

„Ich, Sophie Schumacher, versichere an Eides statt durch meine eigenhändige Unterschrift, dass ich die vorgelegte Dissertation mit dem Thema: „Pathophysiologisch-serologische, bildgebende und klinische Charakteristika der Neuromyelitis Optica“ selbstständig und ohne nicht offengelegte Hilfe Dritter verfasst und keine anderen als die angegebenen Quellen und Hilfsmittel genutzt habe.

Alle Stellen, die wörtlich oder dem Sinne nach auf Publikationen oder Vorträgen anderer Autoren beruhen, sind als solche in korrekter Zitierung (siehe „Uniform Requirements for Manuscripts (URM)“ des ICMJE -*www.**icmje**.org*) kenntlich gemacht. Die Abschnitte zu Methodik (insbesondere praktische Arbeiten, Laborbestimmungen, statistische Aufarbeitung) und Resultaten (insbesondere Abbildungen, Graphiken und Tabellen) entsprechen den URM (s.o) und werden von mir verantwortet.

Meine Anteile an den ausgewählten Publikationen entsprechen denen, die in der untenstehenden gemeinsamen Erklärung mit dem/der Betreuer/in, angegeben sind. Sämtliche Publikationen, die aus dieser Dissertation hervorgegangen sind und bei denen ich Autor bin, entsprechen den URM (s.o) und werden von mir verantwortet.

Die Bedeutung dieser eidesstattlichen Versicherung und die strafrechtlichen Folgen einer unwahren eidesstattlichen Versicherung (§156,161 des Strafgesetzbuches) sind mir bekannt und bewusst.“

_____ _____

Datum Unterschrift

3. Anteilserklärung

Sophie Schumacher hatte folgenden Anteil an den vorgelegten Publikationen:

Publikation 1:

Schumacher S, Pache F, Bellmann-Strobl J, Behrens J, Dusek P, Harms L, K. Ruprecht, P. Nytrova, S. Chawla, T. Niendorf, I. Kister, F. Paul, Y. Ge, J. Wuerfel, T. Sinnecker. Neuromyelitis optica does not impact periventricular venous density versus healthy controls: a 7.0 Tesla MRI clinical study. MAGMA. 2016.

Beitrag im Einzelnen: Mitarbeit an der Erarbeitung des Studienkonzeptes und an der Studiendurchführung; Mitwirkung bei der Patientenakquirierung, Zusammentragen der relevanten klinischen Daten und MRT-Daten der untersuchten Patienten und Kontrollen; eigenständige Analyse der MRT-Daten mit Hilfe der Auswertungssoftware OsiriX; Mithilfe bei der statistischen Analyse; Erstellung eines Entwurfs des Manuskripts und Mitarbeit an der Revision des Manuskripts; Einreichen des endgültigen Manuskripts im Journal *Magnetic Resonance Materials in Physics, Biology and Medicine*

Publikation 2:

Sinnecker T, Schumacher S, Mueller K, Pache F, Dusek P, Harms L, K. Ruprecht, P. Nytrova, S. Chawla, T. Niendorf, I. Kister, F. Paul, Y. Ge, J. Wuerfel. MRI phase changes in multiple sclerosis vs neuromyelitis optica lesions at 7T. Neurol Neuroimmunol Neuroinflamm. 2016.

Beitrag im Einzelnen: Mitwirkung bei der Patientenakquirierung, Zusammentragen der relevanten klinischen Daten und MRT-Daten der untersuchten Patienten und Kontrollen; eigenständige Analyse der MRT-Daten mit Hilfe der Auswertungssoftware OsiriX; Mitarbeit am Entwurf des Manuskripts; Mitarbeit an der Revision des Manuskriptes.

Publikation 3:

Pache F, Zimmermann H, Mikolajczak J, Schumacher S, Lacheta A, Oertel FC, J. Bellmann-Strobl, S. Jarius, B. Wildemann, M. Reindl, A. Waldman, K. Soelberg, N. Asgari, M. Ringelstein, O. Aktas, N. Gross, M. Buttmann, T. Ach, K. Ruprecht, F. Paul, A.U. Brandt, i.c.w.t.N.O.S.G. (NEMOS).

MOG-IgG in NMO and related disorders: a multicenter study of 50 patients. Part 4: Afferent visual system damage after optic neuritis in MOG-IgG-seropositive versus AQP4-IgG-seropositive patients. J Neuroinflammation. 2016.

Beitrag im Einzelnen: Mitwirkung bei der Patientenakquirierung; Betreuung der Patienten während der Studienvisite und Mitarbeit bei der Erhebung der klinischen Daten; Mitarbeit an der Revision des Manuskriptes.

Unterschrift, Datum und Stempel des betreuenden Hochschullehrers

_____

Unterschrift der Doktorandin

_____

4. Druckexemplare der ausgewählten Publikationen

Schumacher S, Pache F, Bellmann-Strobl J, Behrens J, Dusek P, Harms L, K. Ruprecht, P. Nytrova, S. Chawla, T. Niendorf, I. Kister, F. Paul, Y. Ge, J. Wuerfel, T. Sinnecker. Neuromyelitis optica does not impact periventricular venous density versus healthy controls: a 7.0 Tesla MRI clinical study. MAGMA. 2016.

Impact-Factor (2016): 1,718

Eigenfaktor Score (2016): 0,00283

(Seite 32-38)

Schumacher S, Pache F, Bellmann-Strobl J, Behrens J, Dusek P, Harms L, K. Ruprecht, P. Nytrova, S. Chawla, T. Niendorf, I. Kister, F. Paul, Y. Ge, J. Wuerfel, T. Sinnecker. Neuromyelitis optica does not impact periventricular venous density versus healthy controls: a 7.0 Tesla MRI clinical study. MAGMA. 2016.

https://doi.org/10.1007/s10334-016-0554-3

Sinnecker T, Schumacher S, Mueller K, Pache F, Dusek P, Harms L, K. Ruprecht, P. Nytrova, S. Chawla, T. Niendorf, I. Kister, F. Paul, Y. Ge, J. Wuerfel.

MRI phase changes in multiple sclerosis vs neuromyelitis optica lesions at 7T. Neurol Neuroimmunol Neuroinflamm. 2016.

Impact-Factor (2016): 8,32

Eigenfaktor Score (2016): 0,11484

(Seite 40-44)

MRI phase changes in multiple sclerosis vs neuromyelitis optica lesions at 7T

OPEN

Tim Sinnecker, MD
Sophie Schumacher
Katharina Mueller, MD
Florence Pache, MD
Petr Dusek, MD
Lutz Harms, MD
Klemens Ruprecht, MD
Petra Nytrova, MD
Sanjeev Chawla, MD
Thoralf Niendorf, PhD
Ilya Kister, MD
Friedemann Paul, MD
Yulin Ge, MD
Jens Wuerfel, MD

Correspondence to
Dr. Paul:
friedemann.paul@charite.de

ABSTRACT

Objective: To characterize paramagnetic MRI phase signal abnormalities in neuromyelitis optica spectrum disorder (NMOSD) vs multiple sclerosis (MS) lesions in a cross-sectional study.

Methods: Ten patients with NMOSD and 10 patients with relapsing-remitting MS underwent 7-tesla brain MRI including supratentorial T2*-weighted imaging and supratentorial susceptibility weighted imaging. Next, we analyzed intra- and perilesional paramagnetic phase changes on susceptibility weighted imaging filtered magnetic resonance phase images.

Results: We frequently observed paramagnetic rim-like (75 of 232 lesions, 32%) or nodular (32 of 232 lesions, 14%) phase changes in MS lesions, but only rarely in NMOSD lesions (rim-like phase changes: 2 of 112 lesions, 2%, $p < 0.001$; nodular phase changes: 2 of 112 lesions, 2%, $p < 0.001$).

Conclusions: Rim-like or nodular paramagnetic MRI phase changes are characteristic for MS lesions and not frequently detectable in NMOSD. Future prospective studies should ask whether these imaging findings can be used as a biomarker to distinguish between NMOSD- and MS-related brain lesions. *Neurol Neuroimmunol Neuroinflamm* 2016;3:e259; doi: 10.1212/NXI.0000000000000259

GLOSSARY

ICC = intraclass correlation; **MS** = multiple sclerosis; **NMOSD** = neuromyelitis optica spectrum disorder; **SWI** = susceptibility weighted imaging; **T2*w** = T2*-weighted.

Neuromyelitis optica spectrum disorders (NMOSD) and multiple sclerosis (MS) are distinct autoimmune CNS diseases with sometimes overlapping clinical phenotypes.[1] Since treatment options for these 2 CNS diseases differ considerably,[1] the distinction between NMOSD and MS is of high clinical relevance. Recently, new international consensus diagnostic criteria were proposed for NMOSD emphasizing the role of MRI and aquaporin-4 immunoglobulin G antibody testing.[2] Notwithstanding this success, the distinction of NMOSD vs MS can still be challenging in current clinical practice. Ultra-high field MRI at 7 tesla (T) has improved the detection and morphologic characterization of brain lesions by visualizing a central intralesional vein and a T2*-weighted (T2*w) hypointense rim around many MS lesions.[3,4] Contrarily, these imaging features are only rarely depictable in NMOSD lesions.[3,4] At 3T, susceptibility-induced MRI phase signal changes were reported to be specific for MS in contrast to other neurologic disorders such as migraine, antiphospholipid syndrome, and Parkinson disease.[5] Inspired by these findings, we rescanned previously reported patients with NMOSD at 7T[3] and included additional NMOSD cases to describe MRI phase signal changes in NMOSD vs MS lesions in a cross-sectional study.

From the NeuroCure Clinical Research Center (T.S., S.S., K.M., F. Pache, F. Paul, J.W.), Clinical and Experimental Multiple Sclerosis Research Center (L.H., K.R., F. Paul), and Department of Neurology (L.H., K.R., F. Paul), Charité–Universitaetsmedizin Berlin; Institute of Neuroradiology (P.D., J.W.), Universitaetsmedizin Goettingen, Germany; Department of Neurology and Center of Clinical Neuroscience (P.D., P.N.), Charles University in Prague, 1st Faculty of Medicine and General University Hospital in Prague, Czech Republic; Berlin Ultrahigh Field Facility (T.N., J.W.), Max Delbrueck Center for Molecular Medicine, Berlin; Experimental and Clinical Research Center (T.N., F. Paul, J.W.), Charité–Universitaetsmedizin Berlin and Max Delbrueck Center for Molecular Medicine, Berlin, Germany; Department of Radiology (S.C., Y.G.), and Multiple Sclerosis Care Center, Department of Neurology (I.K.), NYU School of Medicine, New York, NY; and Medical Imaging Analysis Center AG (T.S., J.W.), Basel, Switzerland. T.S. is currently with Universitätsspital Basel, Switzerland.

Funding information and disclosures are provided at the end of the article. Go to Neurology.org/nn for full disclosure forms. The Article Processing Charge was paid by the authors.

METHODS

Study participants. Ten patients with NMOSD underwent ultra-high field MRI at 7T. Inclusion criteria were diagnosis of NMOSD as defined by the current international consensus diagnostic criteria for NMOSD,[2] age of at least 18 years, and no contraindications to 7T MRI. Four of these patients have been previously reported in a 7T MRI study on T2*w lesion morphology[3] and were rescanned. Nine patients with NMOSD were seropositive for aquaporin-4 immunoglobulin G. Ten patients with relapsing-remitting MS as defined by the current panel criteria[6] were selected from a research database of the NeuroCure Clinical Research Center as controls. More details are presented in table 1.

The study was approved by the local ethics committee (EA 1/054/09). Written consent was obtained from all participants before examination.

MRI acquisition. Ultra-high field MRIs were acquired using a 7T Siemens whole body scanner (Magnetom; Siemens, Erlangen, Germany) by applying a 24-channel receive head coil (Nova Medical, Wilmington, MA) equipped with a birdcage volume coil used for transmission. The imaging protocol included supratentorial 2-dimensional T2*w fast low angle shot (echo time = 25.0 milliseconds [ms], repetition time = 1,820 ms, spatial resolution = 0.5 × 0.5 × 2 mm^3, supratentorial coverage, number of slices = 35) and supratentorial 3-dimensional gradient echo flow-compensated susceptibility weighted imaging (SWI) (echo time = 14 ms, repetition time = 25 ms, flip angle = 12°, spatial resolution = 0.5 × 0.5 × 1.0 mm^3) yielding magnitude, SWI-filtered phase and reconstructed SWI images.

Table 1 Demographic details

	NMOSD	RRMS
No.	10	10
Female, n	10	5[a]
Age, y, mean ± SD	47 ± 12	40 ± 7[b]
Range	30-69	26-49
Disease duration,[c] y, mean ± SD	8 ± 7	6 ± 4[d]
Range	1-29	0-12
EDSS score, median	3.75	1.5[e]
Range	1.5-6.0	0-2.5
NMOSD, n	10	NA
NMO	3	NA
ON	0	NA
LETM	7	NA

Abbreviations: EDSS = Expanded Disability Status Scale; LETM = longitudinally extensive transverse myelitis; NA = not applicable; NMO = neuromyelitis optica; NMOSD = NMO spectrum disorder; ON = optic neuritis; RRMS = relapsing remitting multiple sclerosis.
[a] $p = 0.010$, Pearson χ^2 test to assess differences in sex between patients with NMOSD and RRMS.
[b] $p = 0.043$, Mann–Whitney U test to assess differences in age between patients with NMOSD and RRMS.
[c] Disease duration = time since first symptoms.
[d] $p = 0.853$, Mann–Whitney U test to assess differences in disease duration between patients with NMOSD and RRMS.
[e] $p = 0.001$, Student t test to assess differences in the EDSS between patients with NMOSD and RRMS.

Image analysis. MRIs were analyzed by a trained investigator (S.S.) blinded to clinical details (diagnosis, Expanded Disability Status Scale score, age, sex) using the OsiriX software package (version 3.8.1; OsiriX Foundation, Geneva, Switzerland). First, all hyperintense brain lesions larger than 3 mm in diameter were marked on T2*w images. The 3-mm cutoff was used to ensure an optimal characterization of the lesion morphology. T2*w lesions outside of the field of view of SWI-phase images were excluded from further analyses.

Next, each existent T2*w lesion was marked on phase images in a side-by-side analysis.

Hereby, the existence of phase changes in or around brain lesions was noted and grouped into 4 categories: (1) lesions with paramagnetic (positive) phase changes in the center of the lesions that are nodular in appearance, (2) lesions with paramagnetic (positive) phase changes at the edge of the lesions that are rim-like in appearance, (3) lesions without any intralesional phase changes, and (4) other lesions with intralesional phase changes not meeting these criteria. The latter were termed "lesions with unspecific phase changes" (figure). Since our scanner uses a left-handed system, a paramagnetic (positive) phase shift corresponds to a hyperintense or "bright" area on phase images. Phase changes that were clearly related to a blood vessel were excluded.

In addition, a lesion with a central vessel within the inner third of the lesion on axial T2*w images was classified as a perivascular lesion by an expert reader regarding the 3-dimensional shape of the lesion and the vessels.

Statistical analysis and interrater reliability. All analyses were performed using IBM SPSS Statistics (version 20; IBM, Armonk, NY). The p values <0.05 were considered significant. Because of the exploratory nature of the study, no adjustments for multiple comparisons were made. Group differences in age, disease duration, existence of a central vein, and intralesional phase changes between NMOSD and MS were assessed using a nonparametric Mann–Whitney U test. Pearson χ^2 was used to assess sex differences, and Student t-test was used to investigate group differences in the Expanded Disability Status Scale. In addition, 10 randomly selected patients with MS or NMOSD were reanalyzed by a second blinded investigator (K.M.) to assess interrater reliability. For this reason, intraclass correlation (ICC) was calculated as a 2-way mixed test of average measures using the consistency model.

RESULTS

In total, we detected 112 brain lesions in patients with NMOSD, and 232 brain lesions were visualized in patients with MS on supratentorial T2*w images.

Next, rim-like or nodular paramagnetic (positive) intralesional phase changes were analyzed (figure). In MS, 32 of 232 lesions (14%) in 7 of 10 patients were characterized by a nodular paramagnetic (positive) phase shift and thus appeared "hyperintense" on magnetic resonance (MR) phase images corresponding to a hypointense signal on T2*w and/or SWIs (lesion category I; figure, A).

Furthermore, a distinct rim-like paramagnetic (positive) phase shift was visible in 75 of 232 MS lesions (32%) in all but one patient with MS (lesion category II; figure, B).

Contrarily, the vast majority of NMOSD lesions were neither characterized by nodular (2 of 112 lesions, 2%, $p < 0.001$) nor rim-like intralesional phase changes (2 of 112 lesions, 2%, $p < 0.001$; table 2).

Figure Lesion morphology of NMOSD vs MS lesions

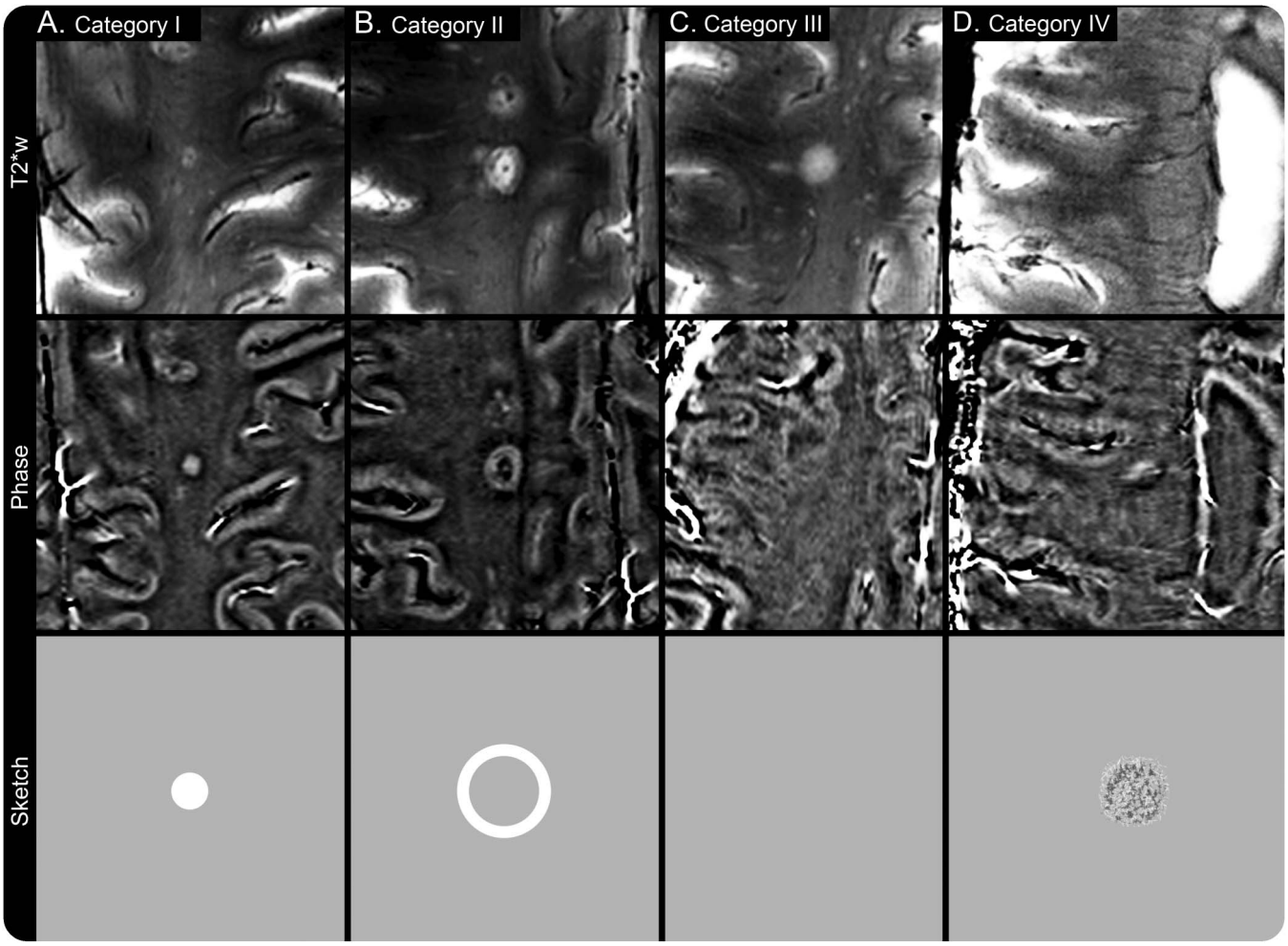

In this study, the existence of phase changes in or around brain lesions was noted and grouped into 4 categories. The figure shows examples of MS (A, B, D) and NMOSD (C) lesions imaged using T2*w and phase MRI. In the bottom row, a schematic is presented for each type of lesion illustrating ideal theoretic phase image appearance. Briefly, category I lesions (A) are characterized by paramagnetic (positive) phase changes in the center of the lesions that are nodular in appearance. Category II lesions (B) show paramagnetic (positive) phase changes at the edge of the lesions that are rim-like in appearance, and category III lesions (C) do not exhibit any intralesional phase changes. Finally, lesions with intralesional phase changes not meeting these criteria are category IV lesions (D). In this example (D), the MS lesion appears to have a small T2*w hypointense rim, but the corresponding phase changes are inconclusive and were thus categorized into lesion category IV. In addition, note the existence of a central vein in the center of the MS lesions (A, B, D) and the absence of such a vessel in the neuromyelitis optica lesion (C). MS = multiple sclerosis; NMOSD = neuromyelitis optica spectrum disorder; T2*w = T2*-weighted.

A significant proportion of lesions in patients with NMOSD (107 of 112 lesions, 96%) or MS (116 of 232 lesions, 50%) did not show any MRI phase changes (lesion category III; figure, C), and a total number of 9 MS and 1 NMOSD lesions presented with rather unspecific MRI phase changes (lesion category IV; figure, D).

In addition, the existence of an intralesional central vein was analyzed on T2*w images. As reported previously,[3,4] a central vein was typically visible in the inner third of MS lesions (193 of 232 lesions, 83%) but only rarely existent in NMOSD lesions (28 of 112 lesions, 25%, $p < 0.001$). The morphology of NMOSD and MS lesions is detailed in table 2.

Interrater reliability. Interrater reliability was assessed in a subgroup of 10 randomly selected patients. ICC was >0.8 for lesion count (ICC = 0.90), the number of lesions with a central vein (ICC = 0.95), and the number of lesions with rim-like (ICC = 0.96) or nodular (ICC = 0.84) phase changes indicating good interrater reliability of these parameters.

DISCUSSION In this study, we compared the morphology of NMOSD vs MS lesions on high spatial resolution SWI-filtered phase images and observed distinct lesion characteristics that were nearly exclusively found in MS but not in NMOSD lesions. Thus, this work adds to the ongoing discussion[5] on the diagnostic value of phase white matter signal abnormalities in differentiating MS from other diseases.

In MS, the source of the phase contrast in or around lesions remains speculative, but iron-rich

Table 2 Lesion morphology on gradient echo images

	Lesion count[a]	Lesions with nodular positive phase changes	Lesions with rim-like positive phase changes	Lesions without phase alterations	Lesions with unspecific phase alterations	Perivascular[b] lesions
NMOSD						
No.	112	2	2	107	1	28
Mean ± SD	11 ± 13	0.2 ± 0.4	0.2 ± 0.4	11 ± 13	0.1 ± 0.3	3 ± 4
Range	1–35	0–1	0–1	1–35	0–1	0–11
RRMS						
No.	232	32	75	116	9	193
Mean ± SD	23 ± 15	3 ± 3	8 ± 10	12 ± 12	1 ± 2	19 ± 13
Range	2–50	0–8	0–33	0–40	0–6	2–41
p	0.063	0.015	<0.001	0.481	0.247	<0.001

Abbreviations: NMOSD = neuromyelitis optica spectrum disorder; RRMS = relapsing remitting multiple sclerosis.
[a] Lesion count = total number of lesions detectable on T2*-weighted images.
[b] Perivascular = visibility of a small central vein within the lesion center.

macrophages or microglia,[7] solutes, proteins, antibodies, cytokines, and immune cells have been hypothesized to cause rim-like phase changes around MS lesions.[8]

Nodular phase changes—a feature of another proportion of MS lesions as reported previously[9]—were discussed to be caused by iron deposits as a consequence of, e.g., dying iron-rich oligodendrocytes,[10] perivascular hemoglobin leakage,[11] or a loss of diamagnetic myelin.[12]

In NMOSD, such nodular or rim-like paramagnetic phase changes were virtually absent. These differences may represent variant patterns of lesion evolution or iron metabolism between MS and NMOSD.[13] In MS, evidence has emerged that brain iron metabolism is altered since iron accumulates, e.g., in the basal ganglia.[14] In alignment with a previous study that failed to identify abnormal iron deposits in the basal ganglia of patients with NMOSD,[15] our data suggest that NMOSD is not associated with alteration in brain iron metabolism, but histopathologic confirmation is needed.

Some limitations of this study of a small sample size need to be addressed. The NMOSD group was older than the MS group, which may have influenced our results since the magnetic susceptibility of (MS) brain lesions decreases with aging of the lesion.[16] Most important, lesions within the brainstem, spinal cord, and optic nerves could not be analyzed, and brain lesions typical for NMOSD[17] were not present in our NMOSD cohort. Thus, the existence of any MRI phase changes in these lesions remains unknown. From a technical point of view, signal inhomogeneities were present on 7T T2*w images, and automated procedures to determine the total lesion volume were thus not performed. Finally, we cannot exclude that differences in lesion count or volume between the subgroups may have influenced our results.

In conclusion, paramagnetic intralesional phase changes were virtually absent in NMOSD but frequently detectable in MS. Future work should address the question of whether these imaging findings in or around lesions can indeed be used as a biomarker to better distinguish MS from NMOSD.

AUTHOR CONTRIBUTIONS

T.S., P.D., L.H., K.R., T.N., I.K., F. Paul, Y.G., and J.W.: study concept and design. T.S., F. Pache, P.D., P.N., and J.W.: acquisition of data. T.S., S.S., and K.M.: analysis. T.S., S.S., K.M., F. Pache, P.D., L.H., K.R., P.N., S.C., T.N., I.K., F. Paul, Y.G., and J.W.: interpretation. T.S., S.S., K.M., F. Pache, P.D., L.H., K.R., P.N., S.C., T.N., I.K., F. Paul, Y.G., and J.W.: critical revision of the manuscript for important intellectual content. T.S., L.H., K.R., T.N., I.K., F. Paul, Y.G., and J.W.: study supervision.

ACKNOWLEDGMENT

This work was supported by the Guthy-Jackson Charitable Foundation, the German Research Foundation (DFG Exc 257 to F.P.), and the German Ministry for Education and Research (Competence Network Multiple Sclerosis) to F.P. and K.R. Our technicians and study nurses Antje Els, Susan Pikol, Cynthia Kraut, and Gritt Stoffels gave invaluable support.

STUDY FUNDING

This work was supported by the Guthy-Jackson Charitable Foundation, the German Research Foundation (DFG Exc 257), and the Competence Network Multiple Sclerosis.

DISCLOSURE

T. Sinnecker received travel funding from Bayer, Teva, Novartis, Genzyme. S. Schumacher and K. Mueller report no disclosures. F. Pache received travel funding from Genzyme, Bayer, Biogen Idec, ECTRIMS, received research support from Charite–Universitaetsmedizin Berlin, Berlin Institute of Health, KKNMS–Bundesministerium für Bildung und Forschung, Novartis. P. Dusek received research support from the Ministry of Health of the Czech Republic. L. Harms served on the scientific advisory boards for Novartis, Sanofi/Genzyme, Roche, Biogen, received travel funding and/or speaker honoraria from Novartis, Biogen Idec, Merck Serono, Bayer HealthCare, Grifols, Teva. K. Ruprecht served on the scientific advisory board for Sanofi-Aventis/Genzyme, Novartis,

Roche, received travel funding and/or speaker honoraria from Bayer HealthCare, Biogen Idec, Merck Serono, Sanofi-Aventis/Genzyme, Teva Pharmaceuticals, Novartis, Guthy Jackson Charitable Foundation, is an associate editor for *PLoS One*, received publishing royalties from Elsevier, received research support from Novartis, German Ministry of Education and Research. P. Neytrova and S. Chawla report no disclosures. T. Niendorf received travel funding from Siemens Healthcare, Erlangen Germany, was a guest editor for *Magnetic Resonance Materials in Physics, Biology and Medicine*, is the founder and CEO of MRI.TOOLS GmbH, received research support from Siemens Healthcare, Erlangen Germany, Helmholtz Association. I. Kister served on the advisory board for Biogen Idec, consulted for Biogen Idec, received research support from Biogen Idec, Serono, Novartis, Guthy-Jackson Charitable Foundation, National Multiple Sclerosis Society. F. Paul served on the scientific advisory board for Novartis, MedImmune, received travel funding and/or speaker honoraria from Bayer, Novartis, Biogen Idec, Teva, Sanofi-Aventis/Genzyme, Merck Serono, Alexion, Chugai, MedImmune, Shire, is an academic editor for *PLoS One*, is an associate editor for *Neurology® Neuroimmunology & Neuroinflammation*, has consulted for Sanofi/Genzyme, Biogen Idec, MedImmune, Shire, Alexion, received research support from Bayer, Novartis, Biogen Idec, Teva, Sanofi-Aventis/Genzyme, Alexion, Merck Serono, German Research Council, Werth Stiftung of the City of Cologne, German Ministry of Education and Research, Arthur Arnstein Stiftung Berlin, Arthur Arnstein Foundation Berlin, Guthy-Jackson Charitable Foundation, National Multiple Sclerosis Society of the United States. Y. Ge received research support from NIH, National MS Society. J. Wuerfel served on the advisory boards for Novartis, Biogen, Genzyme, received travel support from Novartis, and speaker honoraria from Bayer, Biogen Idec, Novartis, is the CEO of MIAC AG, received research support from the German Ministry of Education and Research, German Ministry of Economy, University Medicine Goettingen. Go to Neurology.org/nn for full disclosure forms.

Received January 2, 2016. Accepted in final form May 31, 2016.

REFERENCES

1. Jarius S, Ruprecht K, Wildemann B, et al. Contrasting disease patterns in seropositive and seronegative neuromyelitis optica: a multicentre study of 175 patients. J Neuroinflammation 2012;9:14.
2. Wingerchuk DM, Banwell B, Bennett JL, et al. International consensus diagnostic criteria for neuromyelitis optica spectrum disorders. Neurology 2015;85:177–189.
3. Sinnecker T, Dörr J, Pfueller CF, et al. Distinct lesion morphology at 7-T MRI differentiates neuromyelitis optica from multiple sclerosis. Neurology 2012;79:708–714.
4. Kister I, Herbert J, Zhou Y, Ge Y. Ultrahigh-field MR (7 T) imaging of brain lesions in neuromyelitis optica. Mult Scler Int 2013;2013:398259.
5. Hagemeier J, Heininen-Brown M, Gabelic T, et al. Phase white matter signal abnormalities in patients with clinically isolated syndrome and other neurologic disorders. AJNR Am J Neuroradiol 2014;35:1916–1923.
6. Polman CH, Reingold SC, Banwell B, et al. Diagnostic criteria for multiple sclerosis: 2010 revisions to the McDonald criteria. Ann Neurol 2011;69:292–302.
7. Pitt D, Boster A, Pei W, et al. Imaging cortical lesions in multiple sclerosis with ultra-high-field magnetic resonance imaging. Arch Neurol 2010;67:812–818.
8. Absinta M, Sati P, Gaitán MI, et al. Seven-tesla phase imaging of acute multiple sclerosis lesions: a new window into the inflammatory process. Ann Neurol 2013;74:669–678.
9. Bian W, Harter K, Hammond-Rosenbluth KE, et al. A serial in vivo 7T magnetic resonance phase imaging study of white matter lesions in multiple sclerosis. Mult Scler 2013;19:69–75.
10. Hametner S, Wimmer I, Haider L, Pfeifenbring S, Brück W, Lassmann H. Iron and neurodegeneration in the multiple sclerosis brain. Ann Neurol 2013;74:848–861.
11. Bagnato F, Hametner S, Yao B, et al. Tracking iron in multiple sclerosis: a combined imaging and histopathological study at 7 tesla. Brain 2011;134(pt 12):3602–3615.
12. Li W, Wu B, Liu C. Quantitative susceptibility mapping of human brain reflects spatial variation in tissue composition. Neuroimage 2011;55:1645–1656.
13. Brück W, Popescu B, Lucchinetti CF, et al. Neuromyelitis optica lesions may inform multiple sclerosis heterogeneity debate. Ann Neurol 2012;72:385–394.
14. Habib CA, Liu M, Bawany N, et al. Assessing abnormal iron content in the deep gray matter of patients with multiple sclerosis versus healthy controls. AJNR Am J Neuroradiol 2012;33:252–258.
15. Chen X, Zeng C, Luo T, et al. Iron deposition of the deep grey matter in patients with multiple sclerosis and neuromyelitis optica: a control quantitative study by 3D-enhanced susceptibility-weighted angiography (ESWAN). Eur J Radiol 2012;81:e633–e639.
16. Chen W, Gauthier SA, Gupta A, et al. Quantitative susceptibility mapping of multiple sclerosis lesions at various ages. Radiology 2014;271:183–192.
17. Kim HJ, Paul F, Lana-Peixoto MA, et al. MRI characteristics of neuromyelitis optica spectrum disorder: an international update. Neurology 2015;84:1165–1173.

MRI phase changes in multiple sclerosis vs neuromyelitis optica lesions at 7T

Tim Sinnecker, Sophie Schumacher, Katharina Mueller, et al.

Neurol Neuroimmunol Neuroinflamm 2016;3;
DOI 10.1212/NXI.0000000000000259

Pache F, Zimmermann H, Mikolajczak J, Schumacher S, Lacheta A, Oertel FC, J. Bellmann-Strobl, S. Jarius, B. Wildemann, M. Reindl, A. Waldman, K. Soelberg, N. Asgari, M. Ringelstein, O. Aktas, N. Gross, M. Buttmann, T. Ach, K. Ruprecht, F. Paul, A.U. Brandt, i.c.w.t.N.O.S.G. (NEMOS).

MOG-IgG in NMO and related disorders: a multicenter study of 50 patients. Part 4: Afferent visual system damage after optic neuritis in MOG-IgG-seropositive versus AQP4-IgG-seropositive patients. J Neuroinflammation. 2016.

Impact-Factor (2016): 5,102

Eigenfaktor Score (2016): 0,02390

(Seite 46-55)

Pache et al. Journal of Neuroinflammation (2016) 13:282
DOI 10.1186/s12974-016-0720-6

Journal of Neuroinflammation

RESEARCH Open Access

MOG-IgG in NMO and related disorders: a multicenter study of 50 patients. Part 4: Afferent visual system damage after optic neuritis in MOG-IgG-seropositive versus AQP4-IgG-seropositive patients

Florence Pache[1,2†], Hanna Zimmermann[1,2†], Janine Mikolajczak[1], Sophie Schumacher[1], Anna Lacheta[1], Frederike C. Oertel[1], Judith Bellmann-Strobl[1,12], Sven Jarius[3], Brigitte Wildemann[3], Markus Reindl[4], Amy Waldman[5], Kerstin Soelberg[6,7], Nasrin Asgari[6,7], Marius Ringelstein[8], Orhan Aktas[8], Nikolai Gross[9], Mathias Buttmann[10], Thomas Ach[11], Klemens Ruprecht[2], Friedemann Paul[1,2,12†], and Alexander U. Brandt[1*†]; in cooperation with the Neuromyelitis Optica Study Group (NEMOS)

Abstract

Background: Antibodies against myelin oligodendrocyte glycoprotein (MOG-IgG) have been reported in patients with aquaporin-4 antibody (AQP4-IgG)-negative neuromyelitis optica spectrum disorders (NMOSD). The objective of this study was to describe optic neuritis (ON)-induced neuro-axonal damage in the retina of MOG-IgG-positive patients in comparison with AQP4-IgG-positive NMOSD patients.

Methods: Afferent visual system damage following ON was bilaterally assessed in 16 MOG-IgG-positive patients with a history of ON and compared with that in 16 AQP4-IgG-positive NMOSD patients. In addition, 16 healthy controls matched for age, sex, and disease duration were analyzed. Study data included ON history, retinal optical coherence tomography, visual acuity, and visual evoked potentials.

Results: Eight MOG-IgG-positive patients had a previous diagnosis of AQP4-IgG-negative NMOSD with ON and myelitis, and eight of (mainly recurrent) ON. Twenty-nine of the 32 eyes of the MOG-IgG-positive patients had been affected by at least one episode of ON. Peripapillary retinal nerve fiber layer thickness (pRNFL) and ganglion cell and inner plexiform layer volume (GCIP) were significantly reduced in ON eyes of MOG-IgG-positive patients (pRNFL = 59 ± 23 μm; GCIP = 1.50 ± 0.34 mm^3) compared with healthy controls (pRNFL = 99 ± 6 μm, $p < 0.001$; GCIP = 1.97 ± 0.11 mm^3, $p < 0.001$). Visual acuity was impaired in eyes after ON in MOG-IgG-positive patients (0.35 ± 0.88 logMAR). There were no significant differences in any structural or functional visual parameters between MOG-IgG-positive and AQP4-IgG-positive patients (pRNFL: 59 ± 21 μm; GCIP: 1.41 ± 0.27 mm^3; Visual acuity = 0.72 ± 1.09 logMAR). Importantly, MOG-IgG-positive patients had a significantly higher annual ON relapse rate than AQP4-IgG-positive patients (median 0.69 vs. 0.29 attacks/year, $p = 0.004$), meaning that on average a single ON episode caused less damage in MOG-IgG-positive than in AQP4-IgG-positive patients. pRNFL and GCIP loss correlated with the number of ON episodes in MOG-IgG-positive patients ($p < 0.001$), but not in AQP4-IgG-positive patients.

(Continued on next page)

* Correspondence: Alexander.Brandt@charite.de
†Equal contributors
Friedemann Paul and Alexander U Brandt are equally contributing senior authors. Florence Pache and Hanna Zimmermann are equally contributing first authors.
[1]NeuroCure Clinical Research Center (NCRC), Charité – Universitätsmedizin Berlin, Charitéplatz 1, 10117 Berlin, Germany
Full list of author information is available at the end of the article

(Continued from previous page)

Conclusions: Retinal neuro-axonal damage and visual impairment after ON in MOG-IgG-positive patients are as severe as in AQP4-IgG-positive NMOSD patients. In MOG-IgG-positive patients, damage accrual may be driven by higher relapse rates, whereas AQP4-IgG-positive patients showed fewer but more severe episodes of ON. Given the marked damage in some of our MOG-IgG-positive patients, early diagnosis and timely initiation and close monitoring of immunosuppressive therapy are important.

Keywords: Myelin oligodendrocyte glycoprotein antibodies (MOG-IgG), aquaporin-4 antibodies (AQP4-IgG), NMO-IgG, neuromyelitis optica, Devic syndrome, neuromyelitis optica spectrum disorders (NMOSD), optic neuritis, optical coherence tomography, visual evoked potentials, visual acuity, retinal neuro-axonal damage

Background

Myelin oligodendrocyte glycoprotein (MOG) is expressed on the outer surface of oligodendrocytic myelin sheaths, representing approximately 0.05 % of all myelin-constituting proteins [1]. Antibodies against MOG (MOG-IgG) have been detected in a proportion of aquaporin-4 (AQP4)-IgG-seronegative patients with neuromyelitis optica spectrum disorder (NMOSD) phenotype [2–6]. MOG-IgG have further been reported in children with acute and relapsing-remitting inflammatory demyelinating encephalomyelitis as well as in a proportion of adults with inflammatory demyelinating diseases such as optic neuritis (ON) [7–9].

Currently it is debated whether MOG-IgG-associated encephalomyelitis should be classified as an NMOSD subtype or as a separate disease entity [10–12]. MOG-IgG-seropositive patients from NMOSD cohorts can show clinical features of recurrent transverse myelitis and ON, similar to AQP4-IgG-seropositive patients [4]. However, the cellular target of AQP4-IgG is an astrocytic water channel, suggesting a different mechanism of injury from MOG-IgG. This is supported by a recent case study of a MOG-IgG-seropositive patient who showed severe demyelination with no evidence of astrocytopathy [13] and by further brain biopsy case studies [14–16].

ON in NMOSD patients is often severe with marked retinal nerve fiber layer and ganglion cell layer loss, severe visual impairment including blindness, and a high frequency of bilateral events [17, 18]. In around 20 % of affected eyes, macular microcysts are found in the inner nuclear layer as a sign of severe ON-related retinal injury [19, 20]. In comparison, the extent of afferent visual system damage following ON in MOG-IgG-seropositive patients is less well understood.

Some previous studies, employing either structural or clinical assessment of visual function, suggested that MOG-IgG-positive patients have fewer attacks, better recovery from relapses, and less neuro-axonal retinal damage than AQP4-IgG-positive patients [4, 21, 22]. However, it is a potential drawback that observation periods were relatively short and sample sizes low in those studies. Moreover, some included mostly or exclusively Asian patients [4, 22]; this could be relevant in that genetic factors have been proposed to play a role in NMOSD pathogenesis [17]. By contrast, more recent studies by others [23, 24] and us [25] demonstrate that the disease follows a relapsing course in the long run in most MOG-IgG-positive patients.

The objective of this retrospective multicenter study was to investigate visual system damage after ON in a larger cohort of Caucasian patients with MOG-IgG-associated encephalomyelitis and long-term follow-up using a comprehensive assessment of the afferent visual system including structural, functional, and clinical parameters, and to compare it with that in AQP4-IgG-positive NMOSD patients.

Methods

Patients

MOG-IgG-seropositive patients with a history of ON and available optical coherence tomography (OCT) data were recruited from a large retrospective study [25, 26]. Sixteen patients (15 female; mean age 44.0 ± 15.2 years) were enrolled from six university hospitals in Europe (Germany: Berlin, Freiburg, Düsseldorf, Heidelberg, Würzburg; Denmark: Vejle). The inclusion criteria were age ≥18 years, a confirmed history of ON (more than 3 months prior to visual assessments), and seropositivity for MOG-IgG. A MOG-antibody serum titer of ≥1: 160 was classified as positive [26]. Clinical and paraclinical data on disease onset, relapse history, expanded disability status scale (EDSS) [27], visual acuity, OCT, magnetic resonance imaging (MRI), and immunotherapy were retrospectively collected.. Annualized relapse rate was calculated as the ratio of number of attacks and years since disease onset, excluding patients with disease duration of less than 1 year. All patients were of Caucasian descent; all MOG-IgG-positive patients tested seronegative for AQP4-IgG, and vice versa (Table 1). Eight (50 %) MOG-IgG-positive patients had a previous diagnosis of—mainly recurrent—ON, and eight (50 %) had been diagnosed with NMOSD based on the clinical symptoms of ON and myelitis before anti-MOG-IgG was tested.

Table 1 Demographic data

		MOG-IgG	AQP4-IgG	MOG-IgG vs. AQP4-IgG (MWU/Chi^2)
				p
Patients	*N*	16	16	
Age (years)	Mean ± SD	44.0 ± 15.2	43.2 ± 13.9	0.838
Sex (f/m)		15/1	16/0	>0.999
Ophthalmologic comorbidities	*N*	2[a)] (13 %)	0 (0 %)	
Age at onset (years)	Mean ± SD	37.2 ± 15.1	34.7 ± 14.8	0.669
Time since onset (years)	Mean ± SD	6.9 ± 6.5	8.4 ± 6.8	0.287
ON eyes	*N* (%)	29 (91.6 %)	25 (78.1 %)	
Number of ON episodes	Median (range)	4.5 (1–13)	2 (1-4)	**0.012**
Myelitis prevalence	*N* (%)	8 (50 %)	15 (93.8 %)	**0.018**
ARR	Median (range)	1.25 (0.38–7.14)	0.64 (0.17–1.44)	**0.026**
ON ARR	Median (range)	0.69 (0.17–7.14)	0.29 (0.07–0.96)	**0.004**
EDSS	Median (range)	3.0 (1.0–7.5)	4.0 (1.0–6.5)	0.064

Abbreviations: *AQP4-IgG* aquaporin-4 antibody-seropositive NMOSD patients, *ARR* annualized relapse rate, *EDSS* expanded disability status scale, *f* female, *m* male, *MOG-IgG* myelin oligodendrocyte glycoprotein antibody-seropositive patients, *MWU* Wilcoxon-Mann-Whitney *U* test, *ON* optic neuritis, *SD* standard deviation
[a)]Early stage dry macular degeneration in both eyes and suspect for early stage glaucoma, respectively
p-values in bold emphasis depict significant values ($p < 0.05$)

AQP4-IgG-positive NMOSD patients [28] ($n = 16$, all female, mean age 43.2 ± 13.9 years) and healthy controls (HC, $n = 16$, 15 female, mean age 43.9 ± 15.4 years) were randomly selected from the research database of the NeuroCure Clinical Research Center (Charité – Universitätsmedizin Berlin, Berlin, Germany), matched for sex and age on cohort basis. Two MOG-IgG-positive patients had co-occurring ophthalmologic conditions in both eyes: one had early-stage dry macular degeneration, and glaucoma was suspected in the other patient. These two patients and their matched AQP4-IgG-positive patients and HC were included in the case descriptions but excluded from statistical analyses of OCT and visual function parameters. Furthermore, only eyes with a previous ON were included in statistical analyses. The local ethics committees approved the study protocol in accordance with the Declaration of Helsinki (1964) in its currently applicable version. All participants provided informed written consent.

MOG-IgG and AQP4-IgG assay

MOG-IgG antibodies were detected using a live cell-based assay and a fixed cell-based assay, both employing HEK293 cells transfected with human full-length MOG; mock-transfected cells were used as control substrates (see part 1 for details [26]). AQP4-IgG were detected using a commercially available cell-based assay (EUROIMMUN, Lübeck, Germany) [29, 30].

Optical coherence tomography

OCT was performed using the Spectralis SD-OCT device (Heidelberg Engineering, Heidelberg, Germany) with the automatic real time function for image averaging. Peripapillary retinal nerve fiber layer thickness (pRNFL) was derived from a standard ring scan around the optic nerve head (12°, 768 or 1536 A-scans, 16≤ART≤100). A macular volume scan (25° × 30°, 61 vertical or horizontal B-scans, 768 A-scans per B-scan, 9≤ART≤15) was acquired for retinal layer analysis. All scans underwent quality control [31] and post-processing by one experienced rater in a standardized manner. Layer segmentation was performed with the device's software (Eye Explorer 1.9.10.0 with viewing module 6.0.9.0). Automatic segmentation results were carefully checked for errors and corrected if necessary by an experienced rater masked for the diagnosis of the subjects. Combined ganglion cell and inner plexiform layer volume (GCIP), inner nuclear layer volume, and outer retinal layers volume including the outer plexiform and nuclear layer, inner and outer photoreceptor segments, and retinal pigment epithelium, were extracted from a 6-mm-diameter cylinder around the fovea [32]. Furthermore, all scans were examined for macular microcysts [19] and other retinal pathologies. The OCT parameters are visualized in Fig. 1.

Visual function testing

Visual function testing was performed in MOG-IgG-positive and AQP4-IgG-positive patients at the same visit as OCT, except for one patient (see Additional file 1: Table S1). Visual evoked potentials (VEP) were recorded with checkerboard stimulation (1°) with the device routinely used at the sites. P100 peak latency was included in analysis and considered as abnormal when higher than 112 ms [33] or when no clear signal could be evoked. Habitually corrected visual acuity was tested with letter charts obtained as part of routine clinical care

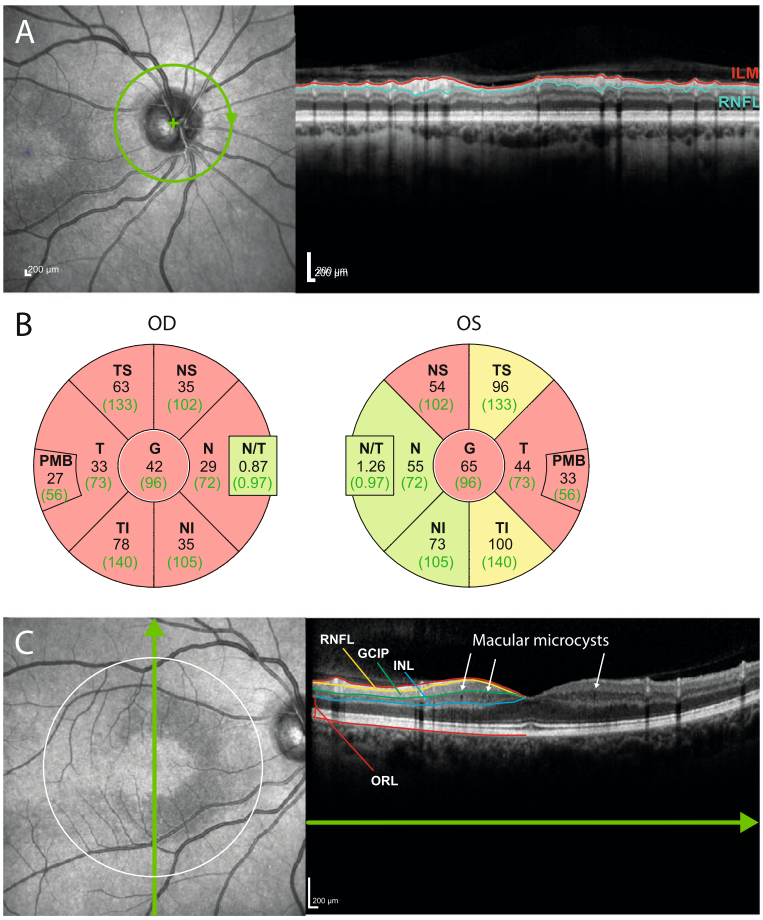

Fig. 1 Sample images from patient 1. **a** Sample images from a peripapillary ring scan. On the *left*, a scanning laser ophthalmoscopy image shows scan positioning (in *green*). On the *right*, an OCT scan shows severe peripapillary retinal nerve fiber layer (pRNFL) loss (between the inner limiting membrane [ILM], shown in *red*, and the lower border, in *turquoise*). **b** Ring-scan data in comparison with normative device data from both eyes of this patient. *Black numbers* display the thickness measurements (in µm) of the subject, *green numbers* the average thickness in the age-matched reference group. Sectors are classified in comparison with the reference group: *green*, thickness values within the 5th and 95th percentile range; *yellow*, 1st to 5th percentile range; *red*, below the 1st percentile. *Abbreviations*: *G* global, *NS* nasal-superior, *N* nasal, *NI* nasal-inferior, *TI* temporal-inferior, *T* temporal, *TS* temporal-superior. **c** Macular scan of the same patient. On the *left*, the dark, sickle-shaped area on and around the macula represents tissue with microcysts in the inner nuclear layer (INL). The *white circle* indicates the 6-mm-diameter cylinder in which intraretinal layers are analyzed. The *green line* with *arrow* shows the scanning position of the OCT scan on the right. Here, the defined layers are the RNFL, the ganglion cell and inner plexiform layer (GCIP), then INL and the outer retinal layers (ORL). Macular microcysts can be seen as small *black dots* in the INL

and converted into logMAR units. A visual acuity of 0.2 logMAR and worse was considered abnormal. When no letter could be recognized by the patient, visual acuity was registered with 2.0 logMAR for finger counting and 3.0 logMAR for hand motion recognition [34].

Data analysis

Statistics were performed in R version 3.1.2 [35] using the packages psych, MASS, geepack and ggplot. Differences in demographics between the cohorts were tested with Pearson chi-square test and non-parametric tests (Mann-Whitney U for two cohorts and Kruskal-Wallis for three cohorts). Comparisons of visual system data between cohorts were performed using generalized estimating equation (GEE) models accounting for intra-subject inter-eye dependencies. GEE results are provided with regression coefficient (B) and standard error (SE). To investigate the extent of damage caused by subsequent ON episodes we employed a linear spline regression model as proposed by Ratchford et al. [36]. Due to the exploratory nature of this study, no correction for multiple comparisons was performed.

Results

The demographic and clinical features of MOG-IgG-positive patients are presented in Table 1 and case-by-case clinical details are provided in Additional file 1: Table S1. One patient had pediatric onset of the disease,

at 6 years of age; her case has been reported in an earlier publication [11]. All other patients had adult onset. All MOG-IgG-positive patients had experienced at least one episode of ON (median 4.5, range 1–13) and, except for one with a short follow-up period (8 months, patient 8), presented with an unequivocally relapsing disease course. Age at onset and disease duration at the time of examination did not differ between MOG-IgG-positive and AQP4-IgG-positive patients (Table 1). Detailed case studies, including therapy, are provided in parts 2 and 3 of this series of articles [25, 37].

OCT and visual function in MOG-IgG-positive ON

Two eyes from two patients had to be excluded from the analysis owing to acute ON at the time of assessment. Thus, 23 eyes from 14 MOG-IgG-positive patients were analyzed at a median time of 16.4 months (range 3–125 months) since the most recent episode of ON. Detailed afferent visual system parameters of all patients are given in Table 2, and case-by-case descriptions are provided in Additional file 2: Table S2.

Reduced pRNFL thickness compared with the manufacturer's normative data was found in 18 of the 23 (78.2 %) ON-affected eyes of the MOG-IgG-positive group (mean 59 ± 23 μm). In addition, two fellow eyes without clinically evident previous ON and with normal VEPs showed reduced RNFL thickness (51 μm and 75 μm, respectively). Five ON eyes (21.7 %) but none of the non-ON eyes had macular microcysts in the inner nuclear layer. Of 20 ON eyes with available VEP data, 12 (60 %) eyes had abnormal P100 latencies—two (10 %) of them despite normal pRNFL—while all four non-ON fellow eyes had normal VEPs. Visual acuity was on average reduced in ON eyes (mean 0.35 ± 0.88 logMAR), with three eyes being legally blind at a visual acuity of 1.0 logMAR and worse. On the other hand, 16 of 23 ON eyes (70 %) preserved visual acuity of 0.1 logMAR or better.

There were no significant differences in OCT and visual function measurements between MOG-IgG-positive patients with a history of both ON and myelitis ($n = 8$) and MOG-IgG-positive patients with a history only of recurrent ON ($n = 8$) (not shown).

Comparison with HC and AQP4-IgG-positive NMOSD patients

We then compared the afferent visual system damage in ON eyes of MOG-IgG-positive patients with age- and sex-matched HC and with ON eyes of AQP4-IgG-positive NMOSD patients (Table 2, Fig. 2). As expected, pRNFL and GCIP were significantly lower than in HC both in the MOG-IgG-positive group (both $p < 0.001$) and in the AQP4-IgG-positive group (both $p < 0.001$). Furthermore, inner nuclear layer volume was significantly greater than HC in the MOG-IgG-positive subgroup ($p = 0.009$), but not in the AQP4-IgG-positive NMOSD subgroup. By contrast, no significant difference was noted between MOG-IgG-positive and AQP4-IgG-positive patients regarding retinal layer measures. Macular

Table 2 Structural and functional data of MOG-IgG-positive patients' ON eyes in comparison to AQP4-IgG-positive patients and control data

	MOG-IgG positive ON ($n = 23$ eyes from 14 subjects)	AQP4-IgG positive ON ($n = 21$ eyes from 14 subjects)	HC ($n = 28$ eyes from 14 subjects)	MOG-IgG positive vs. AQP4-IgG positive (GEE)			MOG-IgG positive vs. HC (GEE)		
				B	SE	*p*	B	SE	*p*
Retinal OCT									
Average pRNFL (μm)	59 ± 23	59 ± 21	99 ± 6	−0.6	7.58	0.94	39.0	6.01	**<0.001**
Nasal pRNFL (μm)	44 ± 21	45 ± 24	74 ± 12	0.2	7.85	0.98	28.6	6.01	**<0.001**
Temporal pRNFL (μm)	44 ± 16	40 ± 15	71 ± 10	−3.0	4.51	0.50	27.6	4.26	**<0.001**
GCIP (mm^3)	1.50 ± 0.34	1.41 ± 0.27	1.97 ± 0.11	−0.10	0.10	0.35	0.47	0.08	**<0.001**
INL (mm^3)	1.03 ± 0.10	1.01 ± 0.11	0.95 ± 0.04	−0.02	0.04	0.55	−0.07	0.03	**0.009**
ORL (mm^3)	4.86 ± 0.26	4.93 ± 0.26	4.73 ± 0.21	0.04	0.09	0.70	−0.13	0.09	0.14
Eyes with macular microcysts (*n*)	5 (21.7 %)	4 (19.0 %)		Chi^2		>0.99			
Visual function									
Visual acuity/logMAR	0.35 ± 0.88	0.72 ± 1.09	-	0.33	0.32	0.30			
Abnormal P100 latency*	12 (57 %)	10 (50 %)	-	Chi^2		0.88			

OCT and visual function results are not including data from the two patients with early stage dry macular degeneration in both eyes and glaucoma, respectively, and their respective AQP4-IgG-positive controls and healthy controls. Furthermore, two eyes of two MOG-IgG positive patients were excluded due to acute ON at time of examination. Explanations: All data are given as mean ± standard deviation (minimum – maximum), if not declared different

AQP4-IgG aquaporin-4 antibody-seropositive NMOSD patients, *GCIP* ganglion cell and inner plexiform layer, *HC* healthy controls, *INL* inner nuclear layer, *ON* eyes with history of optic neuritis, *MOG-IgG* myelin oligodendrocyte glycoprotein antibody-seropositive patients, *ORL* outer retinal layers including layer from outer plexiform layer to Bruch's membrane, *pRNFL* peripapillary retinal nerve fiber layer

p-values in bold emphasis depict significant values ($p < 0.05$)

* VEP data were available for 20 out of 23 ON eyes of MOG-IgG positive patients and 20 out of 21 eyes of AQP4-IgG positive patients

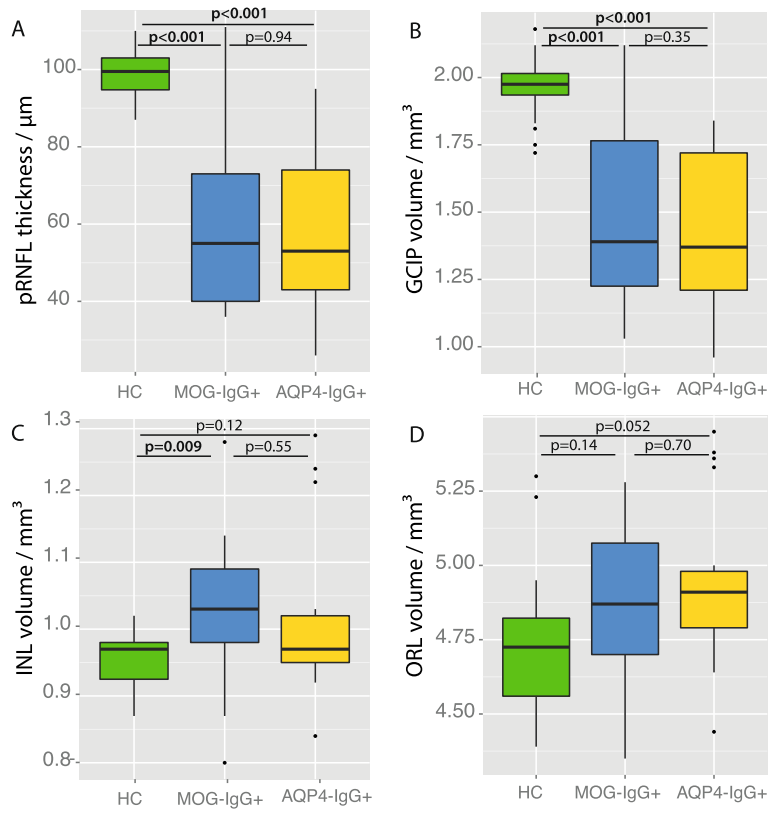

Fig. 2 Retinal layer measures of MOG-IgG-positive and AQP4-IgG-positive ON eyes. *Boxplots* for the comparison of retinal layer measures of the eyes in the healthy control group and the ON eyes of MOG-IgG-positive (MOG-IgG+) and AQP4-IgG-positive (AQP4-IgG+) NMOSD patients. (**a**) Peripapillary retinal nerve fiber layer thickness derived from a ring scan (pRNFL); (**b**-**d**) Intraretinal layer volumes quantified in a 6-mm-diameter cylinder around the fovea centralis: (**b**) ganglion cell and inner plexifom layer volume (GCIP); (**c**) inner nuclear layer volume (INL); (**d**) outer retinal layer volume comprising all layers from outer plexiform layer to Bruch's membrane

microcysts were found in both subgroups in similar prevalence, but differences in microcyst size or extend might have led to a high variability of inner nuclear layer volume values (Table 2). Visual acuity was less impaired in the MOG-IgG-positive subgroup (mean 0.35 ± 0.88 logMAR) than in the AQP4-IgG-positive subgroup (0.72 ± 1.09); however, the difference was not significant ($p = 0.30$).

Of note, the MOG-IgG-positive patients showed a significantly higher annualized relapse rate both for all relapses and—even higher—for ON than the AQP4-IgG-positive patients ($p = 0.026$ and $p = 0.004$, respectively), despite similar disease duration (Table 1).

Retinal damage and number of ON episodes

In MOG-IgG-positive patients, a higher number of ON episodes was associated with more severe pRNFL and GCIP loss (GEE: pRNFL B = −4.9, SE = 1.40, $p < 0.001$; GCIP B = −0.07, SE = 0.02, $p < 0.001$), but not with changes of the inner nuclear layer or outer retinal layers. By contrast, in AQP4-IgG-positive patients the extent of retinal layer changes did not correlate with the number of ON attacks.

In our cross-sectional data, the first ON episode caused a mean pRNFL loss of 12.8 µm ($p = 0.001$) in MOG-IgG-positive patients and 32.8 µm ($p < 0.001$) in AQP4-IgG-positive patients in comparison with HC eyes. In contrast, a second episode of ON caused additional pRNFL loss of 37.8 µm ($p < 0.001$) in MOG-IgG-positive patients and 20.8 µm in AQP4-IgG-positive patients, although that difference was not significant ($p = 0.07$) (Fig. 3). A similar association was found for GCIP volume (data not shown).

Discussion

This study shows that ON in MOG-IgG-positive patients leads to severe pRNFL and GCIP thinning and visual function impairment, the extent of which is comparable to ON in patients with AQP4-IgG. Moreover, it suggests that the damage accrual may be driven by higher relapse rates in MOG-IgG-positive patients, in contrast to more severe ON-associated damage during a single ON episode in AQP4-IgG-positive patients.

Some earlier studies of MOG-IgG-positive patients, which were characterized by relatively short observation

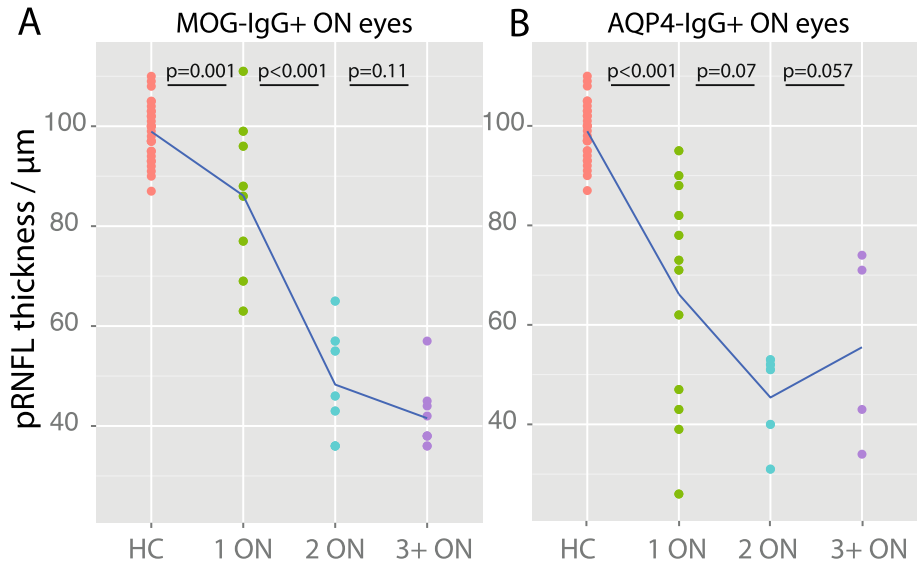

Fig. 3 Retinal nerve fiber layer loss as a function of optic neuritis in MOG-IgG-positive and AQP4-IgG-positive patients. Peripapillary retinal nerve fiber layer (pRNFL) loss caused by sequential episodes of optic neuritis (ON), estimated from cross-sectional data, in comparison with eyes without optic neuritis from the healthy control (HC) cohort. (**a**) ON eyes from MOG-IgG-seropositive patients (MOG-IgG+); (**b**) ON eyes from AQP4-IgG-seropositive patients (AQP4-IgG+). *P*-values were computed with linear regressions

periods, suggested that MOG-IgG-seropositive patients present more often with monophasic disease and have a milder clinical phenotype and better recovery than patients with AQP4-IgG-seropositive NMOSD [4, 5, 38]. By contrast, all but one of our patients showed a relapsing disease course with a high frequency of attacks, protracted ON episodes, and, in some cases, severe visual impairment. In line with our findings, two more recent studies have also demonstrated that MOG-IgG seropositivity is frequently associated with a recurrent disease course in patients with ON [23, 24]. Concerning neuro-axonal damage of the retina, a recent study including 19 MOG-IgG-positive patients reported less retinal nerve fiber and ganglion cell layer damage than in AQP4-IgG-positive patients following ON [22]. As a limitation, however, that study included exclusively monophasic patients. By contrast, in our study we demonstrated that retinal neuro-axonal damage after ON in MOG-IgG-positive patients is at least as severe as in AQP4-IgG-positive NMOSD patients, compared with our own control cohort as well as with previously published AQP4-IgG-positive cohorts [39, 40] when patients with long-term follow-up (mean ~7 years) and, accordingly, relapsing disease course are included in the analysis.

Notably, although average visual function was impaired in relapsing ON of both MOG-IgG-positive and AQP4-IgG-positive patients, some MOG-IgG-positive patients performed comparably well on high-contrast visual acuity testing despite severe neuro-axonal retinal damage: 70 % of ON eyes retained a visual acuity of 0.1 logMAR or better after ON. However, visual acuity was obtained in non-standardized manner as high-contrast letter acuity in clinical routine; thus the reliance on functional testing may underestimate the actual extent of damage to the afferent visual system. The impact of structural damage as demonstrated in the present study should be further investigated with low-contrast letter acuity, color vision testing, visual fields, and quality of life scales.

Our study features strengths and limitations. Among its strengths we count the relatively high number of patients included, given the low prevalence of the disease, the fact that reliable assays for detecting antibodies to full-length human MOG have become available only relatively recently, and the fact that OCT is not yet routinely and generally available. A further potential strength is that our cohort was genetically homogeneous with all patients and controls being of Caucasian origin. As a potential limitation, not all patients were systematically tested for other optic neuropathies, such as Leber's hereditary optic neuropathy (LHON). While a mitochondrial mutation may have contributed to the marked pRNFL thinning in the female patient with pediatric onset of disease (patient 4 in Additional file 1: Table S1), the time course (approximately 10 years before the contralateral eye demonstrated a mild decrease in visual acuity) is unusual for LHON, a condition which typically affects both eyes within months of each other without a relapsing and remitting course. Finally, data were collected retrospectively in a multicenter approach. As a result, additional data, e.g., the Multiple Sclerosis Function Composite or OCT scans obtained during acute optic neuritis, were not available. Moreover, we were not able to systematically correlate optic nerve MRI [23, 41] and OCT in this study,

which would require highly standardized MRI protocols and a prospective study design. However, prospective studies as well as single-center studies in MOG-IgG-positive patients are difficult to perform due to the condition's rarity and the currently limited access to MOG-IgG testing. Moreover, all patients with available data seen at the various centers were included in the analysis, thereby reducing the risk of referral bias. Nonetheless, the preliminary evidence derived from this retrospective exploratory study needs to be confirmed in further prospective and independent studies.

Conclusions

In summary, we demonstrate (a) that a substantial proportion of MOG-IgG-seropositive patients develop retinal neuro-axonal damage; (b) that visual impairment and structural damage increase with the number of attacks and thus with disease duration; and, importantly, (c) that the extent of neuro-axonal damage in MOG-IgG-positive patients with ON is not different from that in patients with AQP4-IgG-positive ON in the long-term course of the disease, i.e., when patients with relapsing rather than monophasic ON are taken into account. Given the marked structural and functional damage in some of our ON patients, early diagnosis, timely initiation of immunosuppressive therapy, and close monitoring of treatment efficacy seem paramount. Although no systematic investigations of drugs for relapse prevention in this condition have yet been conducted, retrospective data on treatment responses (see part 2 of this series [25]), as well as available evidence in favor of a pathogenic role of MOG-IgG [16, 30], suggest that—in accordance with treatment recommendations for AQP4-IgG-positive NMOSD [42]—patients with MOG-IgG-positive ON may benefit from high-dose intravenous methylprednisolone treatment and, possibly, plasma exchange for acute attacks as well as from immunosuppression for attack prevention.

Additional files

Additional file 1: Table S1. Demographic, clinical and serological data. [a)] Early stage dry macular degeneration in both eyes; [b)] Suspected early stage glaucoma. [c)] Visual assessments were performed during acute ON OS. Abbreviations: ON: optic neuritis. VEP P100: visually evoked potential P100 latency. n.e.: not evocable; pRNFL: peripapillary retinal nerve fiber layer thickness. GCIP: combined ganglion cell and inner plexiform layer volume. INL: inner nuclear layer volume. ORL: outer retinal layers volume including layers from outer plexiform layer to Bruch's membrane. (DOCX 21 kb)

Additional file 2: Table S2. Visual evoked potentials, visual acuity, and OCT results. [a)] Protracted relapses were registered as one episode; [b)] Early stage dry macular degeneration in both eyes; [c)] Suspected early stage glaucoma; [d)] Medication other than acute relapse therapy (immunotherapy). Abbreviations: AQP4-IgG = aquaporin-4 antibodies; CRION = chronic relapsing inflammatory optic neuropathy; EDSS = expanded disability status scale; F = female; MOG-IgG = myelin oligodendrocyte glycoprotein antibodies; NMOSD = neuromyelitis optica spectrum disorders; (r)ON = (recurrent) optic neuritis. (DOC 59 kb)

Abbreviations

AQP4-IgG: Aquaporin-4 immunoglobulin G; ARR: Annualized relapse rate; EDSS: Expanded disability status scale; GCIP: Ganglion cell and inner plexiform layer volume; GEE: Generalized estimating equation; LHON: Leber's hereditary optic neuropathy; MOG-IgG: Myelin oligodendrocyte glycoprotein antibody-seropositive patients; MWU: Wilcoxon-Mann-Whitney *U* test; OCT: Optical coherence tomography; ON: Optic neuritis; pRNFL: Peripapillary retinal nerve fiber layer thickness; SD: Standard deviation; SE: Standard error; VEP: Visual evoked potentials

Acknowledgments

BW and SJ are grateful to the Dietmar Hopp Foundation and to Merck Serono for funding research on NMO and related disorders at the Molecular Neuroimmunology Group, Department of Neurology, University of Heidelberg, and to Mrs. Anna Eschlbeck and the Nikon Imaging Center at the University of Heidelberg for excellent technical assistance. FrP would like to acknowledge research support by the German Research Council (DFG Exc 257) and by the Federal Ministry for Education and Research (Competence Network Multiple Sclerosis; N2-ADVISIM). AUB. is grateful to the German Federal Ministry of Economic Affairs and Technology (EXIST-Forschungstransfer RETINEU). MRe would like to thank the Eugene Devic European Network (EDEN) project (ERA–Net ERARE 2; Austrian Science Fund FWF project I916) and the Austrian Federal Ministry of Science, Research and Economy (grant Big Wig MS).

Funding

This work was supported by the Dietmar Hopp Stiftung (BW), Merck Serono (BW), the German Federal Ministry of Education and Research (BMBF/KKNMS, Competence Network Multiple Sclerosis, FrP, KR and OA; N2-ADVISIMS, FrP and AB), the German Federal Ministry for Economic Affairs and Technology (EXIST-Forschungstransfer RETINEU, AB), the German Research Foundation (DFG EXC 257, FP), the Austrian Federal Ministry of Science, Research and Economy (grant Big Wig MS, MRe), the Eugene Devic European Network (EDEN) project (Eurpean Research Area-Net ERARE 2, MRe); the Austrian Science Fund (FWF project I916; MRe).

Availability of data and materials

The datasets during and/or analysed during the current study available from the corresponding author on reasonable request.

Authors' contributions

FIP participated in the design of the study, acquired clinical information, and drafted the manuscript. HZ performed OCT post-processing and statistical analysis and drafted the manuscript. JM acquired OCT and visual function data. SS, AL, and FCO. acquired clinical and visual function data. JBS participated in the design of the study and acquired clinical data. MRe and SJ provided MOG-IgG results and contributed to interpretation of the data. SJ and BW contributed OCT and clinical data and contributed to interpretation of the data. AW contributed to interpretation of the data. KS acquired OCT and visual function data. NA acquired clinical data and contributed to interpretation of the data. MRi acquired OCT, clinical, and visual function data. OA acquired clinical data. NG acquired OCT, clinical, and visual function data. KR participated in the design of the study and contributed to interpretation of the data. MB acquired clinical data, contributed to interpretation of the data, and edited the manuscript. TA acquired OCT and visual function data. FrP contributed to the interpretation of the data and drafted the manuscript. AUB conceived the study and participated in its design and coordination contributed to analysis, and drafted the manuscript. All authors were involved in revising the manuscript for intellectual content and read and approved the final manuscript.

Competing interests

FIP has received a research grant from Novartis Pharmaceuticals and travel grants from Genzyme, a Sanofi company. HZ has received speaking fees from Teva and Bayer. JM has received speaking fees from Teva and Biogen Idec. B.W. has received speaking/consultation honoraria and travel grants from Bayer Healthcare, Biogen Idec, Merck Serono, and Genzyme, a Sanofi company. ATW has received support from the National Institutes of Health and Biogen Idec. MRi has received speaker honoraria from Novartis and Bayer and travel reimbursements from Bayer Schering, Biogen Idec, and Genzyme. OA has received advisor fees or honoraria from Bayer HealthCare,

Biogen, Chugai, Genzyme, MedImmune, Novartis, and Teva; and research support from Bayer HealthCare, Biogen, Novartis, and Teva. KR has received research support from Novartis as well as speaking fees or travel grants from Bayer Healthcare, Biogen Idec, Merck Serono, Sanofi/Genzyme, Teva, Roche, and Novartis. FrP has received research grants and speaker honoraria from Bayer, Teva, Genzyme, Merck, Novartis, and MedImmune and is a member of the steering committee of the OCTIMS study (Novartis). AUB. has received consulting fees from Biogen, Novartis, Teva, Nexus, and Motognosis and funding for research from Novartis and Biogen. All other authors report nothing to disclose. None of the reported disclosures interfered with the present study.

Consent for publication
All participants provided informed written consent for publication.

Ethics approval and consent to participate
The study was approved by the local ethics committees of the participating centers. All participants provided informed written consent.

Author details
[1]NeuroCure Clinical Research Center (NCRC), Charité – Universitätsmedizin Berlin, Charitéplatz 1, 10117 Berlin, Germany. [2]Department of Neurology, Charité – Universitätsmedizin Berlin, Berlin, Germany. [3]Molecular Neuroimmunology Group, Department of Neurology, University of Heidelberg, Heidelberg, Germany. [4]Clinical Department of Neurology, Medical University of Innsbruck, Innsbruck, Austria. [5]Division of Neurology, Children's Hospital of Philadelphia, Pennsylvania, USA. [6]Department of Neurology, Vejle Hospital, Vejle, Denmark. [7]Department of Neurobiology, Institute of Molecular Medicine, University of Southern Denmark, Odense, Denmark. [8]Department of Neurology, Medical Faculty, Heinrich Heine University, Düsseldorf, Germany. [9]Department of Ophthalmology, Medical Faculty, University of Freiburg, Freiburg, Germany. [10]Department of Neurology, University of Würzburg, Würzburg, Germany. [11]Department of Ophthalmology, University of Würzburg, Würzburg, Germany. [12]Experimental and Clinical Research Center, Max Delbrück Center for Molecular Medicine and Charité – Universitätsmedizin Berlin, Berlin, Germany.

Received: 1 April 2016 Accepted: 9 September 2016
Published online: 01 November 2016

References
1. Reindl M, Di Pauli F, Rostásy K, Berger T. The spectrum of MOG autoantibody-associated demyelinating diseases. Nat Rev Neurol. 2013;9:455–61.
2. Mader S, Gredler V, Schanda K, Rostasy K, Dujmovic I, Pfaller K, et al. Complement activating antibodies to myelin oligodendrocyte glycoprotein in neuromyelitis optica and related disorders. J Neuroinflammation. 2011;8:184.
3. Rostásy K, Mader S, Hennes EM, Schanda K, Gredler V, Guenther A, et al. Persisting myelin oligodendrocyte glycoprotein antibodies in aquaporin-4 antibody negative pediatric neuromyelitis optica. Mult Scler J. 2013;19:1052–9.
4. Sato DK, Callegaro D, Lana-Peixoto MA, Waters PJ, Jorge FM, de H, Takahashi T, et al. Distinction between MOG antibody-positive and AQP4 antibody-positive NMO spectrum disorders. Neurology. 2014;82:474–81.
5. Kitley J, Waters P, Woodhall M, Leite MI, Murchison A, George J, et al. Neuromyelitis optica spectrum disorders with aquaporin-4 and myelin-oligodendrocyte glycoprotein antibodies: a comparative study. JAMA Neurol. 2014;71:276–83.
6. Saadoun S, Waters P, Owens GP, Bennett JL, Vincent A, Papadopoulos MC. Neuromyelitis optica MOG-IgG causes reversible lesions in mouse brain. Acta Neuropathol Commun. 2014;2:35.
7. Baumann M, Sahin K, Lechner C, Hennes EM, Schanda K, Mader S, et al. Clinical and neuroradiological differences of paediatric acute disseminating encephalomyelitis with and without antibodies to the myelin oligodendrocyte glycoprotein. J Neurol Neurosurg Psychiatry. 2015;86:265–72.
8. Kim S-M, Woodhall MR, Kim J-S, Kim S-J, Park KS, Vincent A, et al. Antibodies to MOG in adults with inflammatory demyelinating disease of the CNS. Neurol Neuroimmunol Neuroinflammation [Internet]. 2015 [cited 2016 Feb 18];2. Available from: http://www.ncbi.nlm.nih.gov/pmc/articles/PMC4608758/
9. Höftberger R, Sepulveda M, Armangue T, Blanco Y, Rostásy K, Cobo Calvo A, et al. Antibodies to MOG and AQP4 in adults with neuromyelitis optica and suspected limited forms of the disease. Mult Scler J. 2015;21:866–74.
10. Zamvil SS, Slavin AJ. Does MOG Ig-positive AQP4-seronegative opticospinal inflammatory disease justify a diagnosis of NMO spectrum disorder? Neurol Neuroimmunol Neuroinflammation [Internet]. 2015 [cited 2015 Feb 23];2. Available from: http://www.ncbi.nlm.nih.gov/pmc/articles/PMC4309526/
11. Reindl M, Rostasy K. MOG antibody-associated diseases. Neurol Neuroimmunol Neuroinflammation [Internet]. 2015 [cited 2015 Dec 16];2. Available from: http://www.ncbi.nlm.nih.gov/pmc/articles/PMC4309525/
12. Aktas O. Collateral benefit: the comeback of MOG antibodies as a biomarker in neurological practice. J Neurol Neurosurg Psychiatry. 2015;86:243.
13. Ikeda K, Kiyota N, Kuroda H, Sato DK, Nishiyama S, Takahashi T, et al. Severe demyelination but no astrocytopathy in clinically definite neuromyelitis optica with anti-myelin-oligodendrocyte glycoprotein antibody. Mult Scler J. 2015;21:656–9.
14. Spadaro M, Gerdes LA, Mayer MC, Ertl-Wagner B, Laurent S, Krumbholz M, et al. Histopathology and clinical course of MOG-antibody-associated encephalomyelitis. Ann Clin Transl Neurol. 2015;2:295–301.
15. Di Pauli F, Höftberger R, Reindl M, Beer R, Rhomberg P, Schanda K, et al. Fulminant demyelinating encephalomyelitis: Insights from antibody studies and neuropathology. Neurol Neuroimmunol Neuroinflammation. 2015;2:e175.
16. Jarius S, Metz I, König FB, Ruprecht K, Reindl M, Paul F, et al. Screening for MOG-IgG and 27 other anti-glial and anti-neuronal autoantibodies in "pattern II multiple sclerosis" and brain biopsy findings in a MOG-IgG-positive case. Mult Scler J. 2016. doi:10.1177/1352458515622986.
17. Jarius S, Wildemann B, Paul F. Neuromyelitis optica: clinical features, immunopathogenesis and treatment. Clin Exp Immunol. 2014;176:149–64.
18. Bennett JL, de Seze J, Lana-Peixoto M, Palace J, Waldman A, Schippling S, et al. Neuromyelitis optica and multiple sclerosis: Seeing differences through optical coherence tomography. Mult Scler J. 2015;21:678–88.
19. Kaufhold F, Zimmermann H, Schneider E, Ruprecht K, Paul F, Oberwahrenbrock T, et al. Optic Neuritis Is Associated with Inner Nuclear Layer Thickening and Microcystic Macular Edema Independently of Multiple Sclerosis. PLoS One. 2013;8:e71145.
20. Sotirchos ES, Saidha S, Byraiah G, Mealy MA, Ibrahim MA, Sepah YJ, et al. In vivo identification of morphologic retinal abnormalities in neuromyelitis optica. Neurology. 2013;80:1406–14.
21. Martinez-Hernandez E, Sepulveda M, Rostásy K, et al. Antibodies to aquaporin 4, myelin-oligodendrocyte glycoprotein, and the glycine receptor α1 subunit in patients with isolated optic neuritis. JAMA Neurol. 2015;72:187–93.
22. Akaishi T, Sato DK, Nakashima I, Takeshita T, Takahashi T, Doi H, et al. MRI and retinal abnormalities in isolated optic neuritis with myelin oligodendrocyte glycoprotein and aquaporin-4 antibodies: a comparative study. J Neurol Neurosurg Psychiatry. 2016;87(4):446-8.
23. Ramanathan S, Reddel SW, Henderson A, Parratt JDE, Barnett M, Gatt PN, et al. Antibodies to myelin oligodendrocyte glycoprotein in bilateral and recurrent optic neuritis. Neurol Neuroimmunol Neuroinflammation. 2014;1:e40.
24. Chalmoukou K, Alexopoulos H, Akrivou S, Stathopoulos P, Reindl M, Dalakas MC. Anti-MOG antibodies are frequently associated with steroid-sensitive recurrent optic neuritis. Neurol Neuroimmunol Neuroinflammation. 2015;2:e131.
25. Jarius S, Ruprecht K, Kleiter I, Borisow N, Asgari N, Pitarokoili K, et al. MOG-IgG in NMO and related disorders: a multicenter study of 50 patients. Part 2: Epidemiology, clinical presentation, radiological and laboratory features, treatment responses, and long-term outcome. J Neuroinflammation. 2016. doi:10.1186/s12974-016-0718-0.
26. Jarius S, Ruprecht K, Kleiter I, Borisow N, Asgari N, Pitarokoili K, et al. MOG-IgG in NMO and related disorders: a multicenter study of 50 patients. Part 1: Frequency, syndrome specificity, influence of disease activity, long-term course, association with AQP4-IgG, and origin. J Neuroinflammation. 2016. doi:10.1186/s12974-016-0717-1.
27. Kurtzke JF. Rating neurologic impairment in multiple sclerosis: an expanded disability status scale (EDSS). Neurology. 1983;33:1444–52.
28. Wingerchuk DM, Banwell B, Bennett JL, Cabre P, Carroll W, Chitnis T, et al. International consensus diagnostic criteria for neuromyelitis optica spectrum disorders. Neurology. 2015;85:177–89.
29. Jarius S, Probst C, Borowski K, Franciotta D, Wildemann B, Stoecker W, et al. Standardized method for the detection of antibodies to aquaporin-4 based

on a highly sensitive immunofluorescence assay employing recombinant target antigen. J Neurol Sci. 2010;291:52–6.
30. Jarius S, Wildemann B. Aquaporin-4 Antibodies (NMO-IgG) as a Serological Marker of Neuromyelitis Optica: A Critical Review of the Literature. Brain Pathol. 2013;23:661–83.
31. Tewarie P, Balk L, Costello F, Green A, Martin R, Schippling S, et al. The OSCAR-IB Consensus Criteria for Retinal OCT Quality Assessment. PLoS One. 2012;7:e34823.
32. Oberwahrenbrock T, Weinhold M, Mikolajczak J, Zimmermann H, Paul F, Beckers I, et al. Reliability of Intra-Retinal Layer Thickness Estimates. PLoS One. 2015;10:e0137316.
33. Emmerson-Hanover R, Shearer DE, Creel DJ, Dustman RE. Pattern reversal evoked potentials: gender differences and age-related changes in amplitude and latency. Electroencephalogr Clin Neurophysiol. 1994;92:93–101.
34. Holladay JT. Proper method for calculating average visual acuity. J Refract Surg Thorofare NJ. 1997;13:388–91.
35. R Development Core Team. R: a language and environment for statistical computing [Internet]. Vienna, Austria: R Foundation for Statistical Computing; 2010. Available from: http://www.R-project.org
36. Ratchford JN, Quigg ME, Conger A, Frohman T, Frohman EM, Balcer LJ, et al. Optical coherence tomography helps differentiate neuromyelitis optica and MS optic neuropathies. Neurology. 2009;73:302–8.
37. Jarius S, Kleiter I, Ruprecht K, Asgari N, Pitarokoili K, Borisow N, et al. MOG-IgG in NMO and related disorders: a multicenter study of 50 patients. Part 3: Brainstem involvement - frequency, presentation and outcome. J Neuroinflammation. 2016. doi:10.1186/s12974-016-0719-z.
38. Jarius S, Ruprecht K, Wildemann B, Kuempfel T, Ringelstein M, Geis C, et al. Contrasting disease patterns in seropositive and seronegative neuromyelitis optica: A multicentre study of 175 patients. J Neuroinflammation. 2012;9:14.
39. Schneider E, Zimmermann H, Oberwahrenbrock T, Kaufhold F, Kadas EM, Petzold A, et al. Optical Coherence Tomography Reveals Distinct Patterns of Retinal Damage in Neuromyelitis Optica and Multiple Sclerosis. PLoS One. 2013;8:e66151.
40. Bennett JL, de Seze J, Lana-Peixoto M, Palace J, Waldman A, Schippling S, et al. Neuromyelitis optica and multiple sclerosis: Seeing differences through optical coherence tomography. Mult Scler. 2015;21(6):678–88.
41. Galetta SL, Villoslada P, Levin N, Shindler K, Ishikawa H, Parr E, et al. Acute optic neuritis. Neurol Neuroimmunol Neuroinflammation [Internet]. 2015 [cited 2016 Jun 2];2. Available from: http://www.ncbi.nlm.nih.gov/pmc/articles/PMC4516397/
42. Trebst C, Jarius S, Berthele A, Paul F, Schippling S, Wildemann B, et al. Update on the diagnosis and treatment of neuromyelitis optica: Recommendations of the Neuromyelitis Optica Study Group (NEMOS). J Neurol. 2013;261:1–16.

5. Lebenslauf

Mein Lebenslauf wird aus datenschutzrechtlichen Gründen in der elektronischen Version meiner Arbeit nicht veröffentlicht.

6. Komplette Publikationsliste

1. *Schumacher S, Pache F, Bellmann-Strobl J, Behrens J, Dusek P, Harms L, K. Ruprecht, P. Nytrova, S. Chawla, T. Niendorf, I. Kister, F. Paul, Y. Ge, J. Wuerfel, T. Sinnecker. Neuromyelitis optica does not impact periventricular venous density versus healthy controls: a 7.0 Tesla MRI clinical study. MAGMA. 2016.*
   Impact-Factor (2016): 1,718
   Eigenfaktor Score (2016): 0,00283

2. *Sinnecker T, Schumacher S, Mueller K, Pache F, Dusek P, Harms L, K. Ruprecht, P. Nytrova, S. Chawla, T. Niendorf, I. Kister, F. Paul, Y. Ge, J. Wuerfel.*
   MRI phase changes in multiple sclerosis vs neuromyelitis optica lesions at 7T. Neurol Neuroimmunol Neuroinflamm. 2016.
   Impact-Factor (2016): 8,32
   Eigenfaktor Score (2016): 0,11484

3. *Pache F, Zimmermann H, Mikolajczak J, Schumacher S, Lacheta A, Oertel FC, J. Bellmann-Strobl, S. Jarius, B. Wildemann, M. Reindl, A. Waldman, K. Soelberg, N. Asgari, M. Ringelstein, O. Aktas, N. Gross, M. Buttmann, T. Ach, K. Ruprecht, F. Paul, A.U. Brandt, i.c.w.t.N.O.S.G. (NEMOS).*
   MOG-IgG in NMO and related disorders: a multicenter study of 50 patients. Part 4: Afferent visual system damage after optic neuritis in MOG-IgG-seropositive versus AQP4-IgG-seropositive patients. J Neuroinflammation. 2016.
   Impact-Factor (2016): 5,102
   Eigenfaktor Score (2016): 0,02390

7. Danksagung

Meine Danksagung wird aus datenschutzrechtlichen Gründen in der elektronischen Version meiner Arbeit nicht veröffentlicht.